REPORT

TO THE

NATIONAL AERONAUTICS AND SPACE ADMINISTRATION

SEMIANNUAL STATUS REPORT #15

for

GRANT NAGW-533

LABORATORY EVALUATION AND APPLICATION OF MICROWAVE ABSORPTION PROPERTIES UNDER SIMULATED CONDITIONS FOR PLANETARY ATMOSPHERES

Paul G. Steffes, Principal Investigator

November 1, 1990 through April 30, 1991

Submitted by

Professor Paul G. Steffes
School of Electrical Engineering
Georgia Institute of Technology
Atlanta, GA 30332-0250
(404) 894-3128

TABLE OF CONTENTS

		Page
I.	INTRODUCTION AND SUMMARY	1
II.	OUTER PLANETS STUDIES	5
III.	VENUS STUDIES	12
IV.	PUBLICATIONS AND INTERACTIONS WITH OTHER INVESTIGATORS	17
V.	CONCLUSION	18
VI.	REFERENCES	20
VII.	APPENDICES	21

I. INTRODUCTION AND SUMMARY

Radio absorptivity data for planetary atmospheres obtained from spacecraft radio occultation experiments and earth-based radio astronomical observations can be used to infer abundances of microwave absorbing atmospheric constituents in those atmospheres, as long as reliable information regarding the microwave absorbing properties of potential constituents is available. The use of theoretically-derived microwave absorption properties for such atmospheric constituents, or using laboratory measurements of such properties under environmental conditions which are significantly different than those of the planetary atmosphere being studied, often leads to significant misinterpretation of available opacity data. For example, laboratory measurements performed by Joiner et al. (1989), under Grant NAGW-533, have shown that the millimeter-wave capacity of ammonia between 7.5 mm and 9.3 mm and also at the 3.2 mm wavelength is best described by a different lineshape than was previously used in theoretical predictions. The recognition of the need to make such laboratory measurements of simulated planetary atmospheres over a range of temperatures and pressures which correspond to the altitudes probed by both radio occultation experiments and radio astronomical observations, and over a range of frequencies which correspond to those used in both radio occultation experiments and radio astronomical observations, has led to the development of a facility at Georgia Tech which is capable of making such measurements. It has been the goal of this investigation to conduct such measurements and to apply the results to a wide range of planetary observations, both spacecraft and earth-based, in order to determine the identity and abundance profiles of constituents in those planetary atmospheres.

One key activity in the first half of this grant year has continued to be laboratory measurements of the microwave and millimeter-wave properties of the simulated atmospheres of the outer planets and their satellites. However, we have also focussed on development of a radiative transfer model of the Jovian atmosphere at wavelengths from 1 mm to 10 cm. This model utilizes our laboratory data and has also been used to evaluate the need for laboratory measurements of other possible absorbers. This modeling effort has led us to conduct a laboratory measurement of the millimeter-wave opacity of hydrogen sulfide (H_2S) under simulated Jovian conditions. Since our modeling effort suggested that it was possible to determine limits on the abundance of H_2S in the atmosphere of Jupiter using a medium resolution observation at 1.4 mm, an observation of Jupiter was conducted in November, 1990, from the Caltech Submillimeter Observatory (CSO) in Hawaii. Descriptions of the modeling effort, the laboratory experiment, and the observation is given in Section II, and in Appendix B which is a preprint of a paper entitled "Modeling of the Millemeter-Wave Emission of Jupiter Utilizing Laboratory Measurements of Ammonia (NH_3) Opacity" by Joiner and Steffes, which has been submitted to the Journal of Geophysical Research: Planets.

An important source of information regarding the Venus atmosphere is the increasing number of high-resolution millimeter-wavelength emission measurements which have been recently conducted. (See, for example, de Pater et al., 1991) Correlative studies of these measurements with Pioneer-Venus radio occultation measurements (Jenkins and Steffes, 1991) and our longer wavelength emission measurements (Steffes et al., 1990) have provided new ways for characterizing temporal and spatial variations in the abundance of both gaseous H_2SO_4 and SO_2,

and for modeling their roles in the subcloud atmosphere. However, unambiguous results require that we have dependable knowledge of the microwave and millimeter-wave opacity of gaseous and liquid H_2SO_4, and of gaseous SO_2 under Venus conditions.

While some laboratory measurements of the microwave absorption properties of gaseous SO_2 under simulated Venus conditions were made at 13 cm and 3.6 cm wavelengths by Steffes and Eshleman (1981), no measurements have been made at shorter wavelengths. Since the 1.35 cm wavelength appeared to be one of the better wavelengths for measuring the sub-cloud SO_2 abundance (Steffes et al., 1990), we have conducted laboratory measurements of the 1.35 cm (and 13 cm) opacity of gaseous SO_2. The results and application of this work were discussed in the previous Annual Report (includes Seminannual Status Report #14) for Grant NAGW-533 (11/1/89 - 10/31/90). However, during the first half of this grant year we have also conducted laboratory measurements of the absorptivity of gaseous SO_2 at the 3.2 mm wavelength under simulated Venus conditions. These measurements are described in Section III of this report.

Likewise, we have recently completed laboratory measurements of the millimeter-wave dielectric properties of liquid H_2SO_4, in order to model the effects of the opacity of the clouds of Venus on the millimeter-wave emission spectrum. This laboratory experiment and its results are described in Appendix C which is a preprint of a paper entitled "Laboratory Measurement of the Millimeter-Wave Properties of Liquid Sulfuric Acid (H_2SO_4)" by Fahd and Steffes, which has been submitted to the Journal of Geophysical Research: Planets.

In the second half of this grant year we intend to complete the analysis of our observations of the 1.4 mm emission spectrum of Jupiter. By using the results of our laboratory measurements of the 1.4 mm opacity of gaseous H_2S, combined with our radiative transfer model already developed for Jupiter, we hope to establish limits on the abundance and distribution of gaseous H_2S in the Jovian atmosphere. We will also begin construction of the laboratory apparatus for measurement of the millimeter-wave opacity from gaseous H_2SO_4 under simulated Venus conditions. This is an especially difficult task given the high temperatures required to obtain enough H_2SO_4 vapor so as to be able to measure its opacity, and the high pressures characteristic of the Venus atmosphere.

Finally, we intend to pursue an integrated multi-spectral analysis of Venus atmospheric data employing: 1) recent Pioneer-Venus radio occultation data for 13 cm opacity in the Venus atmosphere (ref. Jenkins and Steffes, 1991); 2) recent earth-based observations of the microwave (ref. Steffes et al., 1990) and millimeter-wave (ref. de Pater et al., 1991) emission from Venus, and 3) recent earth-based and spaced-based observations of the I.R. emission from Venus. Our study will also establish requirements for additional laboratory measurements, especially in the I.R. We are also studying the possibility of directly monitoring the signals from the Galileo Jupiter Probe with an earth-based radio telescope so that we could obtain another independent measurement of radio opacity at a localized position within the Jovian atmosphere.

II. OUTER PLANETS STUDIES

1 Measurement of (H_2S) Opacity at G-Band

1.1 Laboratory Configuration

A block diagram of the system used to measure H_2S absorption is shown in Figure 1. The G-Band CW signal (~218 GHz) is generated by doubling a W-Band (~109 GHz) klystron tube source. The klystron power supply provides modulation by varying the voltage on the reflector of the klystron. The variation in frequency using this technique is less than 0.5%. Since the pressure-broadened H_2S line is several GHz wide, absolute frequency stability is not necessary. A sample of the signal from the klystron is taken by a 20 dB coupler and downconverted to an IF of about 800 MHz by a harmonic mixer. A microwave source phase locked to a microwave frequency counter provides the LO for the mixer. The frequency and stability of the IF signal is monitored with a high resolution spectrum analyzer. The frequency of the klystron can be calculated from the precise measurement of the IF and LO frequencies using the spectrum analyzer and frequency counter.

High gain horn antennas are used to transmit and receive the G- band signal which passes through a 71 cm glass cell. A G-Band detector converts the received millimeter-wave signal to a voltage which is measured with a lock in amplifier. A 5 cm piece of WR-5 waveguide (f_c = 168 GHz) acts as a high pass filter to prevent any leakage of the fundamental or first harmonic (~ 109 GHz) through the doubler from being detected. A highpass filter (f_c = 300 GHz) was used to measure the signal level of the third harmonic (~ 327 GHz). The power from the third harmonic was found to be more than 30 dB down from the second harmonic. Thus, the detector is measuring power from only the desired harmonic.

Reflections occur at the cell boundaries due to the different dielectric constants of the air outside the cell, gas mixture in the cell, and lens material at the cell boundary. In order to measure the absorption due to the H_2S gas mixure, the power or voltage on the detector is first measured with the H_2S mixture in the cell. The power is then measured in the cell filled with a gas mixture of 90% hydrogen and 10% helium. This mixture has a similar index of refraction as that of the H_2S gas mixture. Thus, the reflections occurring at the cell boundaries will be similar for both gas mixtures. The absorption due to the hydrogen and helium mixure is negligible. The attenuation due to the H_2S mixure can be inferred from the ratio of the voltages measured with the two gas mixtures in the cell. This approach ensures that the drop in signal level is due only to absorption and not changes in reflection at the cell interfaces.

A pre-mixed, constituent analyzed gas mixture (Matheson) is used in all experiments. This mixture consists of 78.79% H_2, 9.28% He and 11.93% H_2S. A relatively high mixing ratio of H_2S is needed in order to measure absorption in the cell. The uncertainty in this mixture is $\pm 2\%$ of the stated component mixing ratio. The experiments take place at ambient temperature (296K) and at a total pressure of 2 atm.

The main source of uncertainty in this experiment is due to power drift in the klystron source. Power and frequency drift occur as the temperature of the klystron varies. Although the klystron is mounted on a large heat sink to reduce power and frequency drift, the output power exhibits a sinusoidal drift. By carefully characterizing the sinusoidal drift in power, the error bars have been minimized.

1.2 Experimetal Results

The pressure-broadened linewidth of H_2S in an H_2/He atmosphere can be expressed by

$$\Delta\nu = \left(\frac{T}{T_o}\right)^n \cdot \left[\Delta\nu_{H_2} P_{H_2} + \Delta\nu_{He} P_{He} + \Delta\nu_{H_2S} P_{H_2S}\right] \quad (1)$$

where $\Delta\nu_{HH}$ is the hydrogen-broadened linewidth and n is assumed to be 2/3. The self-broadened linewidths of several H_2S lines, including the $2_{0,2} - 2_{1,1}$ line at 217 GHz, have been measured by Helminger and De Lucia (1977). The reported value of the self-broadened line width of the $2_{0,2} - 2_{1,1}$ line, $\Delta\nu_{H_2S}$, is 9.10 MHz/Torr (6.92 GHz/bar). The helium-broadened linewidth, $\Delta\nu_{He}$ has been measured for the $1_{0,1} - 1_{1,1}$ line of H_2S at 168.8 GHz and at 295K by Wiley *et al.* (1989) and found to be 1.60 MHz/Torr (1.22 GHz/Bar). We assume the same value for the $2_{0,2} - 2_{1,1}$ transition.

The measured absorption at a pressure of 2 atm at room temperature is shown in Figure 2. The solid lines represent the theoretically computed absorption. The line parameters used in the absorption computation are taken from the GEISA line catalog. We use the Van-Vleck Weisskopf lineshape with the line width as given in Equation 1. The absorption in dB/m is calculated for several values of $\Delta\nu_{H_2}$. Visual inspection of Figure 1 reveals that the value of $\Delta\nu_{H_2}$ is approximately 2 ± 0.5 GHz/Bar (2.6 ± 0.7 MHz/Torr).

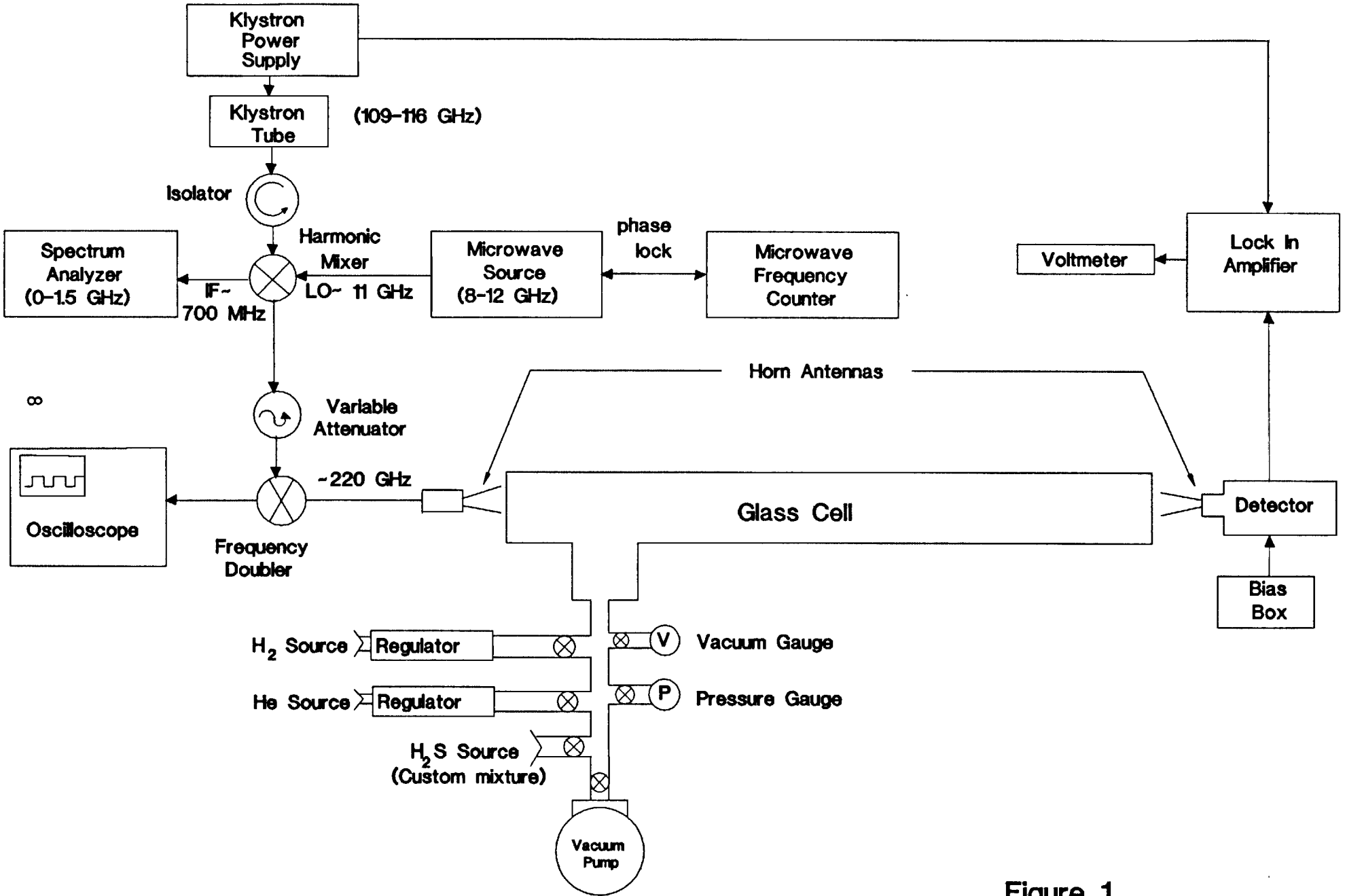
Klystron Power Supply
Klystron Tube
(109-116 GHz)
Isolator
Harmonic Mixer
Spectrum Analyzer (0-1.5 GHz)
IF~ 700 MHz
LO~ 11 GHz
Microwave Source (8-12 GHz)
phase lock
Microwave Frequency Counter
Voltmeter
Lock In Amplifier
Horn Antennas
Variable Attenuator
~220 GHz
Oscilloscope
Frequency Doubler
Glass Cell
Detector
Bias Box
H2 Source
Regulator
He Source
Regulator
H2S Source (Custom mixture)
V
Vacuum Gauge
P
Pressure Gauge
Vacuum Pump

Figure 1

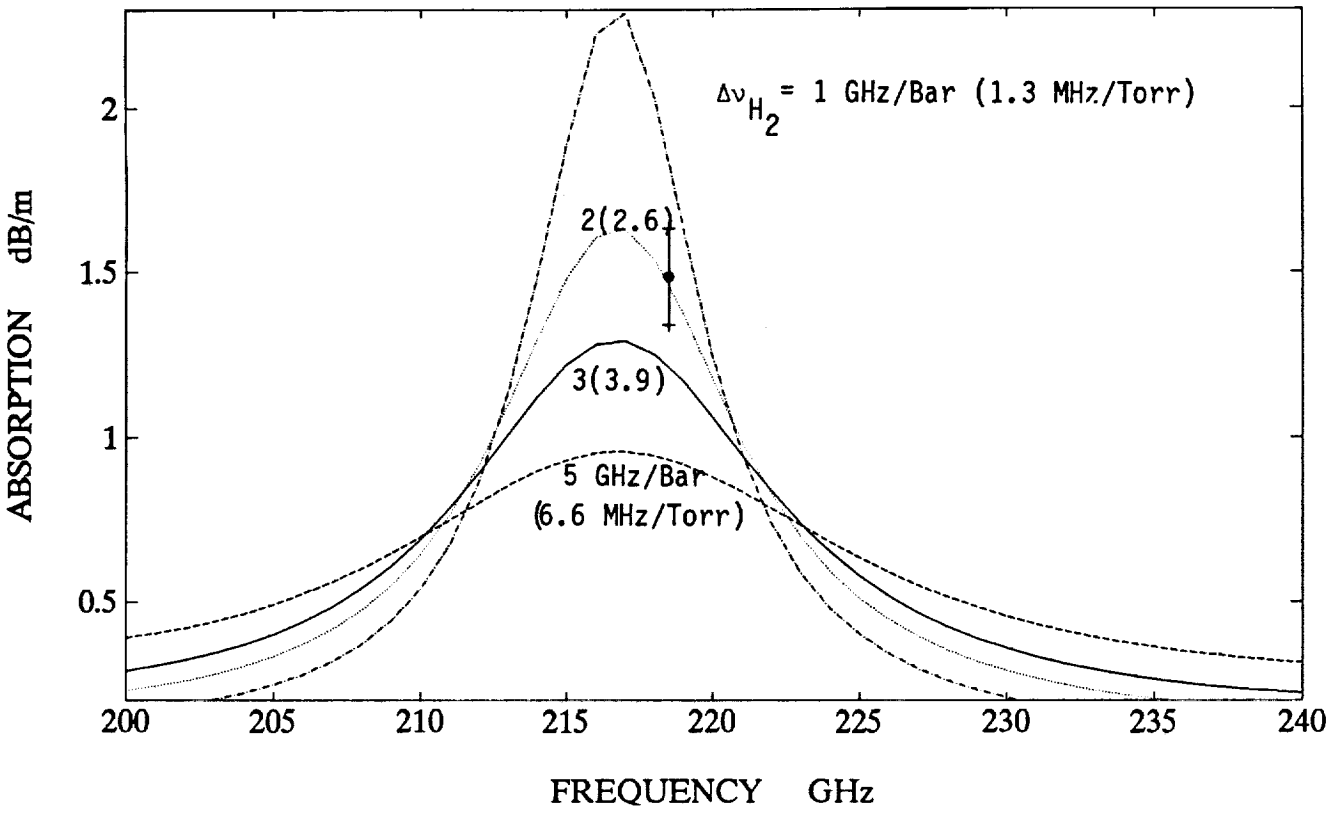

Figure 2: Result from laboratory measurement of the 1.4 mm opacity from H_2S in a H_2/He atmosphere. Note that the results are most consistent with a broadening parameter of 2 GHz/Bar , or 2.6 MHz/Torr.

2. Dual Wavelength Observation of Jupiter at 1.4 mm

2.1 Instrumentation

The observations were made with the 10.4m Caltech Submillimeter Observatory (CSO). The receiver is double side band with a band separation of 2.8 GHz. The receiver (double side band) temperatures measured at 215 and 230 GHz were 220K and 240K respectively. The Acousto-Optic Spectromoeter (AOS) has a total bandwidth of 500 MHz and 1024 channels.

We observed both Jupiter and Mars on November 25, 1990, with the LO centered at 215.3 GHz. The frequency of the $2_{0,2}$ - $2_{1,1}$ transition of H_2S (216.7 GHz) is then centered in the upper sideband. The two planets were observed on November 26, 1990, at a frequency 229.6 GHz. This frequency was chosen so that the CO transition at 230.5 GHz, which has been observed in the spectrum of Mars, would be in between the upper and lower sidebands. Therefore, it would not interfere with the observed continuum level of Mars.

Chopping was accomplished in the position switching mode. In this mode, the antenna is alternately pointed ON the source (planet) and at a position in the sky OFF the source 5' in either the + or - azimuth direction. The telescope remains ON the source and OFF the source for a duration of 10 seconds. One scan of the source is defined as 4 ON/OFF cycles resulting in a total integration time of 80 seconds per scan. A chopper wheel calibration is performed before each scan of the planet. This calibration removes the effects of the earth's atmospheric opacity.

Accurate pointing of the antenna is accomplished by constructing a five point map of the planet in order to calculate the center of the source. After initially

centering the telescope on the planet, the pointing was accurate to better than 4". The telescope was typically repointed after every other scan.

2.2 Calibration

Brightness temperatures of 211.9 and 212.6K are assumed for Mars at 216 and 230 GHz, respectively. These temperatures are based on the models of Rudy (private communication, 1991). The calculated millimeter-wave emission from Mars is assumed to be accurate to within ± 10%.

The temperatures of the planets are corrected for partial filling of the antenna beam using the correction factor in Ulich et. al., (1980). For Jupiter, we use an equatorial radius at the 1 bar level of 71495 km and an ellipticity of 0.065. This value is based on the radio occultation experiment aboard Voyager (Lindal et al., 1986). A value of 3397 km was assumed for the Mars equatorial radius with an ellipticity of 0.0006. These are the same values as those used by Griffin et al. (1986).

Ideally, the observations of Jupiter should be made when the calibrator (Mars) is close to the source (Jupiter) in the sky. In this case, the effects of any time or spatial variation in the earth's atmospheric opacity will be limited. However, good observations of Jupiter relative to Mars can still be made if the atmospheric opacity is relatively stable and both planets are observed at similar elevations.

2.3 Results

Analysis of this data is currently ongoing and should be completed by the end of this grant year.

III. VENUS STUDIES

Laboratory measurements of the opacity of gaseous SO_2 under Venus-like conditions:

Gaseous sulfur dioxide has long been recognized as one of the dominant absorbers present in the middle atmosphere of Venus (Steffes et. al, 1990). To fully understand the role of gaseous SO_2 on the observed millimeter-wave emission from Venus, a knowledge of the absorption of gaseous SO_2 in a CO2 atmosphere at millimeter-wave is necessary. This need has motivated a direct measurement of the opacity of gaseous SO_2 at 3.2 mm.

The experimental approach used to measure the absorptivity of gaseous SO_2 in a CO_2 atmosphere is similar to that previously used by Joiner and Steffes (1991) in determining the millimeter-wave opacity of NH_3 under Jovian-like conditions. A block diagram of the experimental setup is shown in Figure (3). In this setup, a Fabry-Perot resonator shown in Figure (4) is employed to measure the opacity of SO_2 at 94 GHz. The absorptivity is measured by observing the effects of the test gas mixture on the quality factors (Q's) of the Fabry-Perot resonator. For relatively low-loss gas mixtures, the relation between the absorptivity of the gas mixture and its effect on the Q and the transmissivity (t) of a particular resonance is given by:

$$\alpha = \frac{\pi}{\lambda}\left(Q_{mg}^{-1}\left(1-t_g^{-1/2}\right)-Q_{m\theta}^{-1}\left(1-t_\theta^{-1/2}\right)\right)$$

where α is the absorptivity of the gas mixture in Nepers/Km, note: an attenuation constant, or absorption coefficient or absorptivity of 1 Neper/Km =2 optical depths per Km = 8.686 dB/Km where the first notation is the natural form used in electrical engineering,

the second is the prevalent form used in physics and astronomy, and the third is the common (logarithmic) form. Q_{mg} is the measured quality factor with the gas mixture present while Q_{me} is the measured quality factor of the empty resonator. In addition, t_g denotes the transmissivity through the cavity at resonance with the gas mixture loaded while t_e denotes the measured transmissivity without the gas mixture. By using the above expression to calculate the absorption of gaseous SO_2, one can minimize the effect of dielectric loading which may be present in the system.

The results of our measurements are shown in Figure (5). In this figure, the absorption (normalized to mixing ratio) of gaseous SO_2 at two distinct pressures are compared with the theoretically calculated values of the opacity of SO_2 in accordance with the Van-Vleck Weiskopf formalism. As a result, we can state that our measured opacity agrees with the predicted values from the VVW model. These results are extremely important since they show that the f^2 dependence of the opacity of SO_2 which was proposed by Jansen and Poynter (1981) and adopted by Steffes and Eshleman (1981) for frequencies below 100 GHz is not valid.

Currently, we are working on incorporating our measurements into a radiative transfer model in order to investigate the role of SO_2 on the millimeter-wave brightness temperature of Venus.

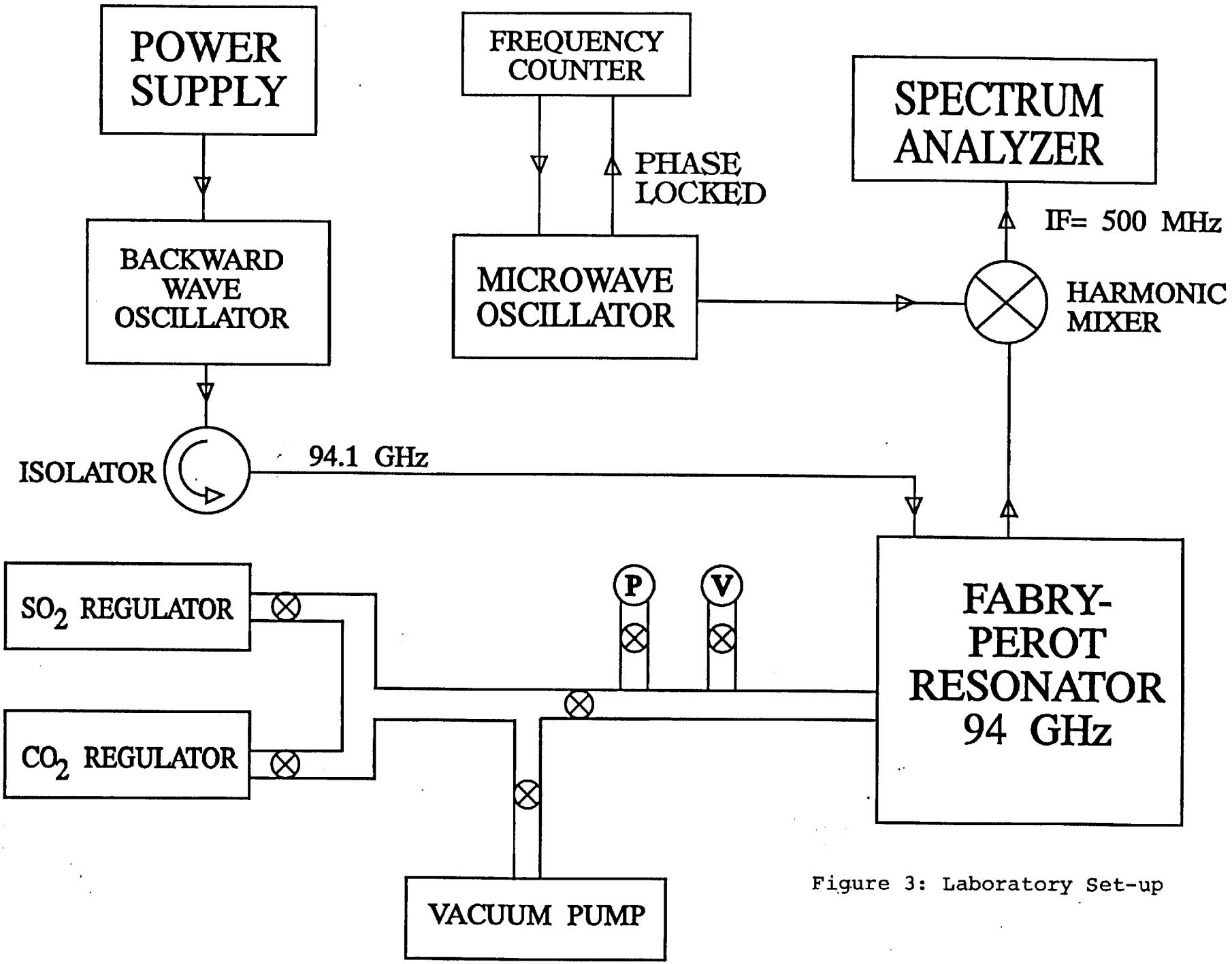

Figure 3: Laboratory Set-up

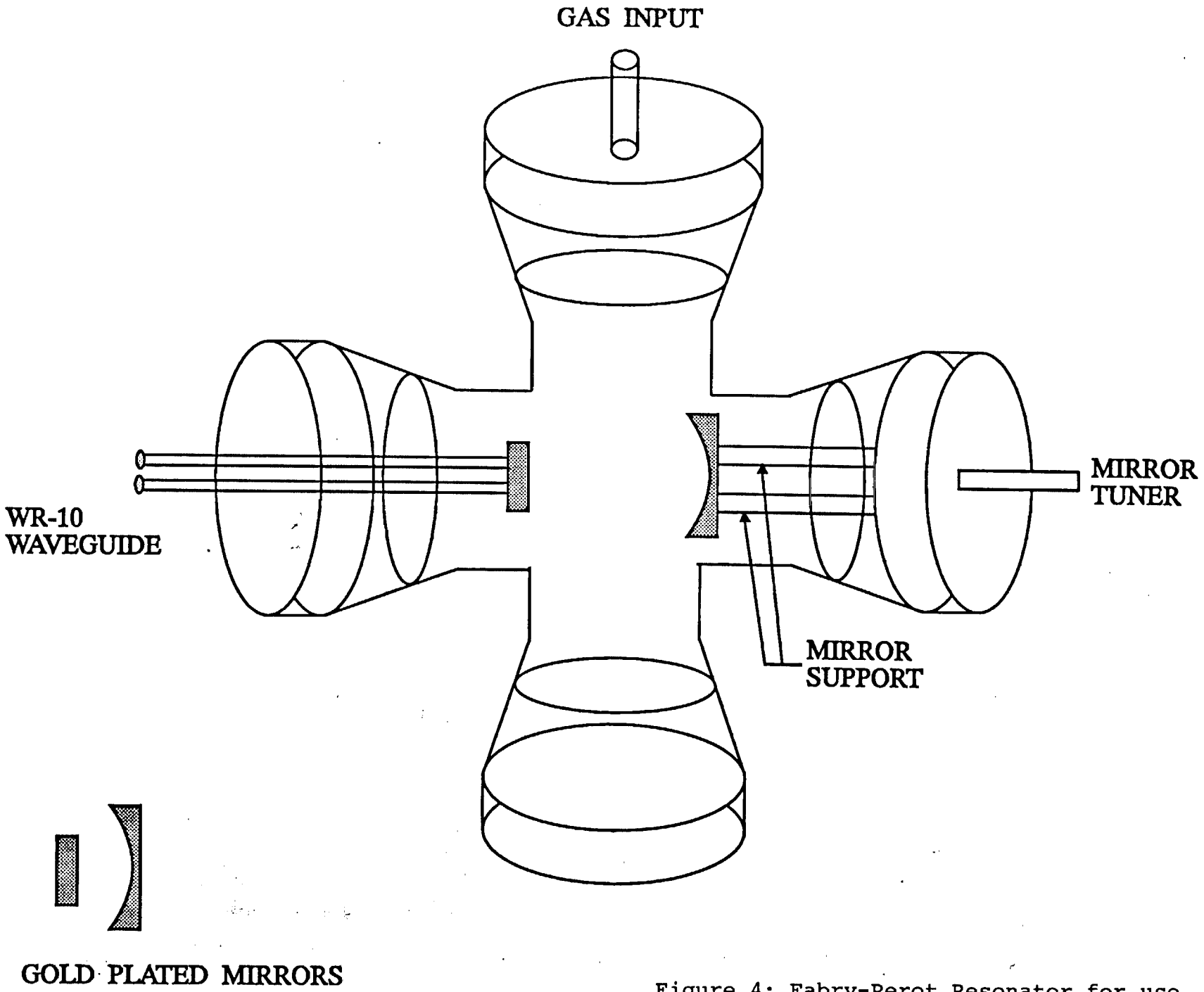

Figure 4: Fabry-Perot Resonator for use at 94 GHz.

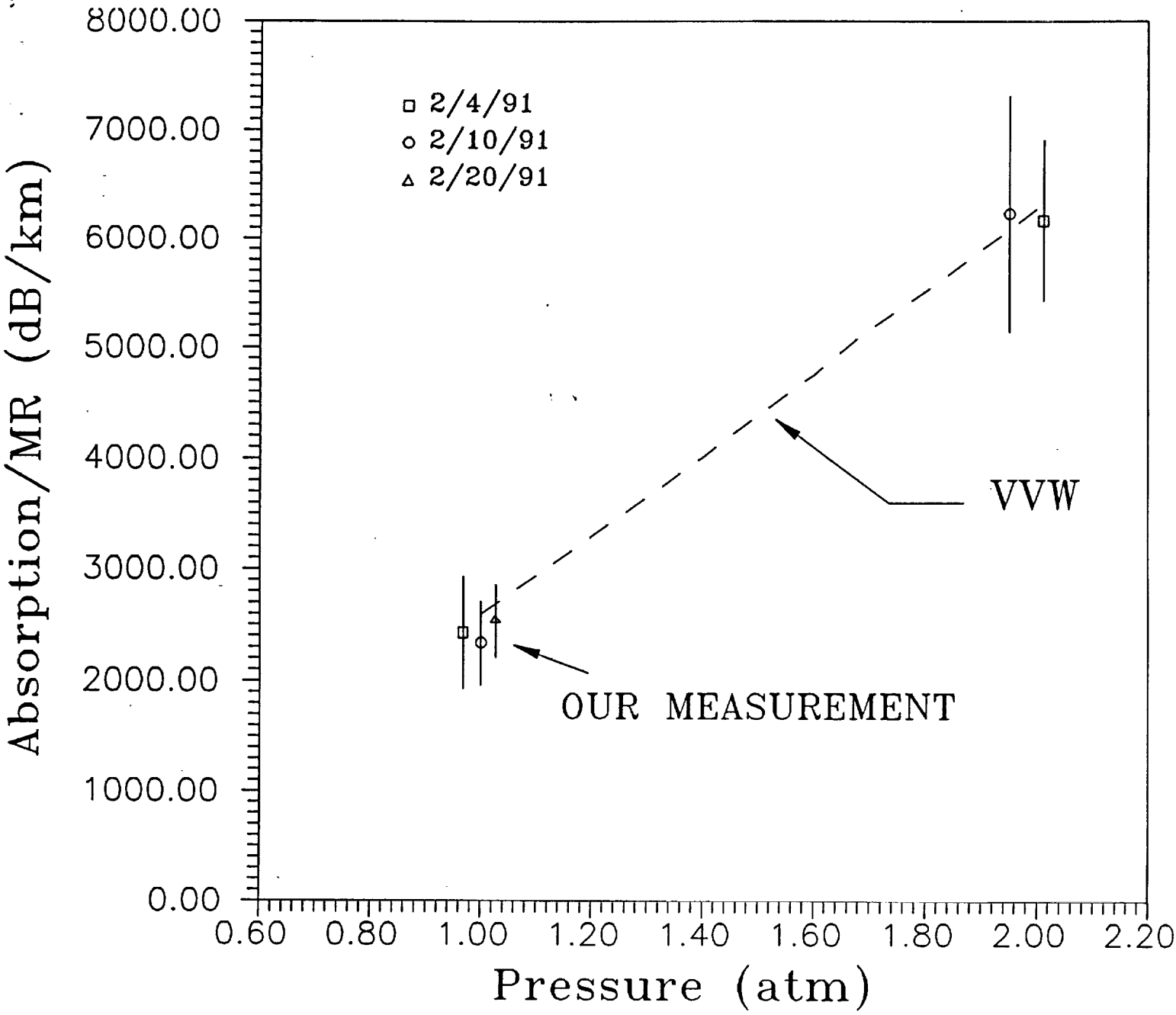

Figure 5: Results for the absorptivity (dB/km) of SO_2 in a CO_2 atmosphere. Note that the results are normalized by SO_2 mixing ratio. This experiment was conducted at a temperature of 293 K.

IV. PUBLICATIONS AND INTERACTION WITH OTHER INVESTIGATORS

After attending the October, 1990, AAS/DPS meeting (Charlottesville, VA) where we presented 4 papers (Fahd and Steffes, 1990a; Fahd and Steffes, 1990b; Joiner and Steffes, 1990; Jenkins and Steffes, 1990; see Appendix A), we prepared and submitted two papers to the new Journal of Geophysical Research: Planets. These papers are to be included in a special issue on Laboratory Research for Planetary Atmospheres. The first is entitled "Modeling of the Millimeter-Wave Emission of Jupiter Utilizing Laboratory Measurements of Ammonia (NH_3) Opacity" by Joiner and Steffes and is attached as Appendix B. The second is entitled "Laboratory Measurement of the Millimeter-Wave Properties of Liquid Sulfuric Acid (H_2SO_4)" by Fahd and Steffes and is attached as Appendix C.

Our work has been complemented by our past involvement in the Pioneer-Venus Guest Investigator Program in which we processed radio occultation data in order to obtain 13 cm absorptivity profiles for the Venus atmosphere (Jenkins and Steffes, 1991). This has kept us in close contact with a large number of Venus investigators. More informal contacts have been maintained with groups at the California Institute of Technology, with the Stanford Center for Radar Astronomy (Drs. V.R. Eshleman, G.L. Tyler, and T. Spilker, regarding Voyager results for the outer planets, and laboratory measurements), and with JPL (Drs. Robert Poynter, Samuel Gulkis, and Michael Klein, regarding radio astronomical observations of the outer planets and Venus). We have also worked with Dr. Imke de Pater (University of California-Berkeley) by using our laboratory measurements of atmospheric gases in the interpretation of radio astronomical observation of Venus and the outer planets. We have also studied possible effects of the

microwave opacity of cloud layers in the outer planets' atmospheres. In this area, we have worked both with Dr. de Pater and with Dr. Paul Romani (Goddard SFC).

In the second half of this grant year, we will again submit results of our latest work to the annual AAS/DPS meeting. We will also submit a paper to the IEEE Transactions on Microwave Theory and Techniques describing our observations of Jupiter and accompanying laboratory measurements of H_2S at the 1.4 mm wavelength. (This will be submitted for a special issue on "Microwaves in Space" commemorating the International Space Year.) Finally, we will prepare and submit a paper to Icarus describing our laboratory measurements of the microwave and millimeter-wave opacity of SO_2, and how the results affect interpretation of the microwave and millimeter-wave emission from Venus.

V. CONCLUSION

In the first half of this grant year we have continued a very active program of laboratory measurements of the microwave and millimeter-wave properties of planetary atmospheric constituents. We have also been involved in observational and interpretive studies of the microwave and millimeter-wave emission from planetary atmospheres. In the second half we intend to complete the analysis of our observations of the 1.4 mm emission spectrum of Jupiter. By using the results of our laboratory measurements of the 1.4 mm opacity of gaseous H_2S, combined with our radiative transfer model already developed for Jupiter, we hope to establish strong limits on the abundance and distribution of gaseous H_2S in the Jovian atmosphere. We will also begin construction of the laboratory

apparatus for measurement of the millimeter-wave opacity from gaseous H_2SO_4 under simulated Venus conditions. This is an especially difficult task given the high temperatures required to obtain enough H_2SO_4 vapor so as to be able to measure its opacity, and the high pressures characteristic of the Venus atmosphere.

Finally, we intend to pursue an integrated multi-spectral analysis of Venus atmospheric data employing: 1) recent Pioneer-Venus radio occultation data for 13 cm opacity in the Venus atmosphere (ref. Jenkins and Steffes, 1991); 2) recent earth-based observations of the microwave (ref. Steffes et al., 1990) and millimeter-wave (ref. de Pater et al., 1991) emission from Venus, and 3) recent earth-based and spaced-based observations of the I.R. emission from Venus. Our study will also establish requirements for additional laboratory measurements, especially in the I.R.

VII. REFERENCES

de Pater, I., F.P. Schloerb, and A. Rudolph 1991. Venus imaged with the Hat Creek Interferometer in the J = 1-0 line. Icarus, in press.

Fahd, A.K. and P.G. Steffes 1990a. Laboratory measurements of the millimeter-wave properties of liquid sulfuric acid (H_2SO_4) between 90 - 200 GHz. Bull. Amer. Astron. Soc. 22, 1035.

Fahd, A.K. and P.G. Steffes 1990b. Laboratory measurement of the 1.3 and 13.3 cm opacity of gaseous SO_2 under simulated conditions of the middle atmosphere of Venus. Bull. Amer. Astron. Soc. 22, 1032.

Griffin, M.J., P.A.R. Ade, G.S. Orton, E.I. Robson, W.K. Gear, I.G. Nolt, and J.V. Radostitz 1986. Submillimeter and millimeter observations of Jupiter. Icarus 65, 244-256.

Helminger, P. and F.C. DeLucia 1977. Pressure broadening of hydrogen sulfide. J. Quant. Spec. Rad. Transfer 17, 751-754.

Jenkins, J.M. and P.G. Steffes 1990. Sulfuric acid vapor profiles for the atmosphere of Venus below the main cloud deck. Bull. Amer. Astron. Soc. 22, 1055.

Jenkins, J.M. and P.G. Steffes 1991. Results for 13 cm absorptivity and H_2SO_4 abundance profiles from the Season 10 (1986) Pioneer-Venus orbiter radio occultation experiment. Icarus 90, 129-138.

Joiner, J., P.G. Steffes, and J.M. Jenkins 1989. Laboratory measurements of the 7.5 - 9.38 mm absorption of gaseous ammonia (NH_3) under simulated Jovian conditions. Icarus 81, 386-395.

Joiner, J. and P.G. Steffes 1990. Study of millimeter-wave absorbing constituents in the Jovian atmospheres. Bull. Amer. Astron. Soc., 22, 1032.

Joiner, J. and P.G. Steffes 1991. Modeling of the millimeter-wave emission of Jupiter utilizing laboratory measurements of ammonia (NH_3) opacity. Submitted to Journal of Geophysical Research: Planets. (Attached, Appendix B).

Lindal, G.F., G.E. Wood, G.S. Levy, J.O. Anderson, D.N. Sweetnam, H.B. Hotz, B.J. Buckles, D.P. Holmes, P.E. Dams, V.R. Eshleman, G.L. Tyler, and T.A. Croft 1981. The atmosphere of Jupiter: An analysis of the Voyager Radio Occultation measurements. J. Geophys. Res. 86, 8721-8727.

Steffes, P.G. and V.R. Eshleman 1981. Laboratory measurements of the microwave opacity of sulfur dioxide and other cloud-related gases under simulated conditions for the middle atmosphere of Venus. Icarus 48, 108-187.

Steffes, P.G. M.J. Klein and J.M. Jenkins 1990. Observations of the microwave emission of Enus from 1.3 to 3.6 cm. Icarus 84, 83-92

Ulich, B.L., J.H. Davis, P.J. Rhodes, and J.M. Hollis 1980. Absolute brightness temperature measurements at 3.5 mm wavelength. IEEE Trans. Ant. Prop., AP-28, No. 3, 367-377.

Wiley, D.R., T.M. Goyette, W.L. Ebenstein, D.N. Bittner, and F.C. DeLucia 1989. Collisionally cooled spectroscopy: pressure broadening below 5K. J. Chem. Phys. 91

VII. APPENDICES

DIVISION FOR PLANETARY SCIENCES ABSTRACT FORM

Run.No._____ Sess.No._____
FOR EDITORIAL USE ONLY

Preferred Mode of Presentation ☒ ORAL ☐ POSTER

PAPER PRESENTED BY ANTOINE K. FAHD
(Please Print, Must be First Author)

SPECIAL INSTRUCTIONS:

35643 GA. TECH. STATION
First Author's Address – Print

ATLANTA, GA. 30332

Antoine K. Fahd
Signature of First Author

Paul G. Steffes
Signature of Introducing Member, if Author is a Nonmember

Phone 404-894-3128

Membership Status (First Author):

DPS-AAS Member ☐ Non-Member ☐ Student ☒

Is your abstract newsworthy, and if so would you be willing to assist our publicity staff with additional material or interviews for reporters.

Yes ☒ No ☐ Maybe ☐

Abstracts must conform to the AAS style as described on the back of this form.

The charge for publication of this abstract in the *Bulletin of the American Astronomical Society* will be included in the registration fee for this meeting.

Deadline for receipt of abstract: August 1, 1990.

SUBMIT ABSTRACT TO: **DPS Abstracts**
Publications Offce, Stephanie Tindell
Lunar & Planetary Institute
3303 NASA Road One
Houston, TX 77058

FOR EDITORIAL USE ONLY

BAAS VOL_____ NO _____199___

Abstract Submitted for the Division for Planetary Sciences, Charlottesville Meeting

Date Submitted _____ Form Version 4/90

23

Appendix A 1

Laboratory measurement of the millimeter-wave properties of liquid sulfuric acid (H_2SO_4) between 90-100 GHz.

A.K. Fahd, P.G. Steffes (Georgia Institute of Technology)

Recent observations of the millimeter-wave emission from Venus at 115 GHz (2.6 mm) have shown significant variations in the continuum flux emission (de Pater et al., in press) which may be attributed to the variability in the abundances of the absorbing constituents in the middle atmosphere of Venus. Such constituents include gaseous H_2SO_4 and SO_2, and liquid H_2SO_4 (the cloud condensate). CO_2 is considered to be the major contributor to the millimeter-wave opacity but its abundance variability is low. Estimating the absorbing properties of any of these constituents at frequencies near 100 GHz is difficult since no laboratory measurements have been reported for Venus-like conditions. It has been proposed that the cloud condensate is the major source of this observed variability in the flux emission. This prediction assumed that the millimeter-wave opacity of liquid sulfuric acid is similar to that of water. However, since the microwave ($\lambda \geq 1$ cm) properties of water are substantially different from sulfuric acid (Cimino, 1982), a laboratory measurement of the complex dielectric constant of liquid H_2SO_4 at millimeter wavelengths is also needed.
Laboratory measurements of the dielectric properties of liquid sulfuric acid between 90-100 GHz have been conducted using a free space transmission setup to measure the complex dielectric constant of liquid sulfuric acid at room temperature for two acid concentrations (99% and 85% by weight). These results, plus a comparison between the opacity of liquid H_2SO_4 and water are presented.

* This work was supported by the Planetary Atmospheres Program of the National Aeronautics and Space Administration under grant NAGW-533.

DIVISION FOR PLANETARY SCIENCES ABSTRACT FORM

Run.No._____ Sess.No._____
FOR EDITORIAL USE ONLY

Preferred Mode of Presentation ☒ ORAL ☐ POSTER

PAPER PRESENTED BY Paul G. Steffes
(Please Print, Must be First Author)

SPECIAL INSTRUCTIONS:
First author is presenting another paper, so second author (DPS-AAS member who is not presenting any other paper) will present

35643 GA. TECH. STATION
First Author's Address -- Print

Anton K. Fahd
Signature of First Author

ATLANTA, GA. 30332

Paul G. Steffes
Signature of Introducing Member, if Author is a Nonmember

Phone 404-894-3128

Membership Status (First Author):

DPS-AAS Member ☐ Non-Member ☐ Student ☒

Is your abstract newsworthy, and if so would you be willing to assist our publicity staff with additional material or interviews for reporters.

Yes ☒ No ☐ Maybe ☐

Abstracts must conform to the AAS style as described on the back of this form.

The charge for publication of this abstract in the *Bulletin of the American Astronomical Society* will be included in the registration fee for this meeting.

Deadline for receipt of abstract: August 1, 1990.

SUBMIT ABSTRACT TO: **DPS Abstracts**
Publications Offce, Stephanie Tindell
Lunar & Planetary Institute
3303 NASA Road One
Houston, TX 77058

FOR EDITORIAL USE ONLY

BAAS VOL_____ NO _____ 199____

24

Laboratory measurements of the 1.3 and 13.3 cm. opacity of gaseous SO_2 under simulated conditions of the middle atmosphere of Venus.

A.K. Fahd, P.G. Steffes (Georgia Institute of Technology)

Gaseous sulfur dioxide has long been recognized as one of the dominant microwave absorbers in the middle atmosphere of Venus (Steffes, Icarus 1985,1990). This has motivated a direct measurement of the opacity of SO_2 at 1.3 and 13.3 cm wavelengths. Although some laboratory measurements of the microwave absorption properties of gaseous SO_2 under simulated Venus conditions were made at 13 and 3.6 cm. wavelengths by Steffes and Eshleman (Icarus, 1981), no measurements have been made at shorter wavelengths specifically at 1.38 cm.

The experimental approach used to measure the microwave absorptivity of gaseous SO_2 in a CO_2 atmosphere is similar to that used previously by Steffes (Icarus, 1985) for characterizing the absorption of gaseous H_2SO_4 in a CO_2 atmosphere. In short, the absorptivity is measured by observing the effects of the test gas mixture on the quality factors (Q's) of the microwave resonances between 2.2 and 22 GHz of two separate cavity resonators. The results at 2.24 GHz are consistent with results from Steffes and Eshleman (Icarus, 1981) in that the measured opacity is at least 50% larger than computed opacity from the Van Vleck-Weisskopf formalism. However, the 21.7 GHz (1.38 cm.) results are quite consistent with the Van Vleck-Weisskopf formalism. This result is extremely important since it shows that the f^2 dependence of SO_2 opacity which was proposed by Jansen and Poynter(Icarus, 1981) and adopted by steffes and Eshleman (Icarus, 1981) for frequencies below 100 Ghz and pressures greater than 1 Bar is not valid. As an application of our measurements, an estimate of the abundance of gaseous SO_2 is made possible by utilizing the Van Vleck-Weisskopf model of gaseous SO_2 along with the 1.35 cm. emission measured by Steffes et al. (Icarus, 1990).

* This work was supported by the Planetary Atmospheres Program of the National Aeronautics and Space Administration under grant NAGW-533.

Abstract Submitted for the Division for Planetary Sciences, Charlottesville Meeting

Date Submitted _____ Form Version 4/90

Appendix A 2

DIVISION FOR PLANETARY SCIENCES ABSTRACT FORM

Run.No._____ Sess.No._____
FOR EDITORIAL USE ONLY

Preferred Mode of Presentation ☒ ORAL ☐ POSTER

PAPER PRESENTED BY Joanna Joiner
(Please Print, Must be First Author)

SPECIAL INSTRUCTIONS:

School of Electrical Engineering
First Author's Address – Print

Joanna Joiner
Signature of First Author

Georgia Institute of Technology

Signature of Introducing Member, if Author is a Nonmember

Atlanta, GA 30332-0250 Phone (404) 894-3128

Membership Status (First Author):

DPS-AAS Member ☒ Non-Member ☐ Student ☒

Is your abstract newsworthy, and if so would you be willing to assist our publicity staff with additional material or interviews for reporters.

Yes ☐ No ☐ Maybe ☒

Abstracts must conform to the AAS style as described on the back of this form.

The charge for publication of this abstract in the *Bulletin of the American Astronomical Society* will be included in the registration fee for this meeting.

Deadline for receipt of abstract: August 1, 1990.

SUBMIT ABSTRACT TO: **DPS Abstracts**
Publications Offce, Stephanie Tindell
Lunar & Planetary Institute
3303 NASA Road One
Houston, TX 77058

FOR EDITORIAL USE ONLY

BAAS VOL_____ NO _____ 199___

Study of Millimeter-wave Absorbing Constituents in the Jovian Atmospheres

J. Joiner, P.G. Steffes (Georgia Institute of Technology)

The millimeter-wave absorption from gaseous ammonia (NH_3) has been previously measured under simulated Jovian conditions. When applied to models of the emission from Jupiter, the results suggested that some other absorber may be present at millimeter wavelengths. We have made measurements of the absorption from gaseous hydrogen sulfide (H_2S) under simulated Jovian conditions near the 1.4 mm rotational line in order to evaluate the pressure broadening effects of hydrogen and helium. We also give new expressions for the millimeter-wave pressure-induced absorption from hydrogen, helium, and methane, absorption from water vapor, potential absorption from cloud condensates and apply these expressions to models of the millimeter-wave emission from the Jovian planets.

*This work was supported by NASA Grant NAGW-533. This material is also based on work supported by NASA through the Georgia Tech Space Grant Consortium.

Abstract Submitted for the Division for Planetary Sciences, Charlottesville Meeting

Date Submitted _____ Form Version 4/90

DIVISION FOR PLANETARY SCIENCES ABSTRACT FORM

Run.No._____ Sess.No._____
FOR EDITORIAL USE ONLY

Sulfuric Acid Vapor Profiles for the Atmosphere of Venus below the Main Cloud Deck

J.M. Jenkins, P.G. Steffes (Georgia Institute of Technology)

Observations of the 1.35 to 3.6 cm emission from Venus have suggested that significant temporal and/or spatial variations in the abundance and distribution of gaseous sulfuric acid below the main cloud layer (48 km and below) may be occurring. To investigate these phenomena, we have processed 13-cm Pioneer-Venus radio occultation data from 19 orbits in 1986 and 1987 to obtain 13-cm absorptivity profiles and sulfuric acid vapor abundance profiles. The data span a range of latitudes from 11°N to 88°N, solar zenith angles from 66° to 160° and probe altitudes as deep as 41 km (above a mean surface radius of 6051.3 km). Statistical uncertainties in the derived profiles have been characterized, allowing us to evaluate the statistical significance of spatial variations in the abundance and distribution of sulfuric acid vapor.

* This work was supported by NASA Grant NAG 2-515. This material is also based on work supported under a National Science Foundation Graduate Fellowship.

Preferred Mode of Presentation [XX] ORAL [ ] POSTER

PAPER PRESENTED BY J.M. Jenkins
(Please Print, Must be First Author)

SPECIAL INSTRUCTIONS:

34260 GA Tech Station
First Author's Address – Print

Atlanta, GA 30332

Signature of First Author

Signature of Introducing Member, if Author is a Nonmember

Phone (404) 894-3128

Membership Status (First Author):

DPS-AAS Member [XX] Non-Member [ ] Student [XX]

Is your abstract newsworthy, and if so would you be willing to assist our publicity staff with additional material or interviews for reporters.

Yes [ ] No [ ] Maybe [XX]

Abstracts must conform to the AAS style as described on the back of this form.

The charge for publication of this abstract in the *Bulletin of the American Astronomical Society* will be included in the registration fee for this meeting.

Deadline for receipt of abstract: August 1, 1990.

SUBMIT ABSTRACT TO: **DPS Abstracts**
Publications Offce, Stephanie Tindell
Lunar & Planetary Institute
3303 NASA Road One
Houston, TX 77058

FOR EDITORIAL USE ONLY

BAAS VOL_____ NO _____ 199___

Abstract Submitted for the Division for Planetary Sciences, Charlottesville Meeting

Date Submitted 7-27-90 Form Version 4/90

Modeling of the Millimeter-wave Emission of Jupiter Utilizing Laboratory Measurements of Ammonia (NH_3) Opacity

JOANNA JOINER AND PAUL G. STEFFES

School of Electrical Engineering, Georgia Institute of Technology, Atlanta, GA 30332-0250

Radiative transfer models which have been used to calculate the millimeter-wave emission from Jupiter do not agree well with the existing radio astronomical observations (*e.g.* dePater and Massie, 1985). This apparent discrepancy has gone largely unexplained due to a lack of laboratory data at these wavelengths coupled with uncertainties in the calibration of existing radio astronomical observations. Previous laboratory measurements of the 7.5 to 9.38 mm opacity from gaseous ammonia (NH_3) by Joiner *et al.* (1989) were inconclusive as to which theoretical lineshape most accuratedly describes the behavior of NH_3 at these wavelengths. We have made additional laboratory measurements of the millimeter-wave opacity of gaseous ammonia at a shorter wavelength (3.2 mm) where the theoretical lineshapes are further separated. The measurements were conducted at a temperature of 210K, at pressures ranging from 1 to 2 atm, and in a mixture consisting of 85.56% hydrogen (H_2), 9.37% helium (He), and 5.07% ammonia (NH_3). We have given a revised formalism for the Ben-Reuven lineshape in order to predict the absorption from NH_3 in an H_2/He atmosphere. We investigate several other potential candidates for millimeter-wave absorption and give revised formalisms for computing their absorption. We have compiled a list of reliable millimeter-wave radio astronomical observations of Jupiter. We compare our revised list of observations to calculated emission spectra which utilize revised expressions for the absorption from NH_3 as well as other opacity sources.

1. Introduction

The millimeter-wave spectrum is a one of the few regions capable of probing beneath the dense cloud layers of Jupiter. The measured emission from Jupiter at microwave frequencies (below 30 GHz) can be well explained by models using various profiles for the abundance of ammonia (NH_3), the dominant absorber at these frequencies. However, when the same models are used to calculate the emission at millimeter wavelengths, a discrepancy is found to exist between the calculated emission and the existing radio astronomical observations (see *e.g.* dePater and Massie, 1985). Because there are several sources of uncertainty in both the observations and the models, inferring information from millimeter-wave spectra of Jupiter is difficult.

One of the largest sources of uncertainty in modeling the millimeter-wave emission from the outer planets involves the calculation of the absorption coefficient of the atmospheric constituents. There are several sources of opacity in the millimeter-wave spectra of Jupiter. The dominant absorber at millimeter wavelengths is gaseous ammonia (NH_3). Another source of millimeter-wave opacity is pressure-induced absorption from hydrogen, helium, and methane. Bezard *et al.* (1983) first demonstrated that gaseous hydrogen sulfide (H_2S), which has yet to be detected on the outer planets, may be contributing to the opacity observed in Jupiter's millimeter-wave spectrum. Both H_2S and H_2O have strong rotational lines at millimeter wavelengths. Cloud particles may provide another source of millimeter-wave opacity. Although molecules such as PH_3, HCN, and CO contain strong absorption lines at millimeter wavelengths, they do not exist in abundances great enough to significantly affect the millimeter-wave spectrum of Jupiter.

Accurate calibration of the radio astronomical observations of the outer planets at millimeter wavelengths is critical if meaningful comparisons are to be made between different observations and between the observations and radiative transfer models. The most frequently used calibrator at these wavelengths is Mars. However, the uncertainty in the modelled flux from Mars is reported to be at least 10% (Griffin *et al.* , 1986) and could be as high as 20% (Orton, *private communication*, 1989). Before the millimeter-wave spectrum of Jupiter is fully understood, better calibration techniques will be needed. In addition, laboratory studies of potential absorbers are needed in order to interpret the measured emission from Jupiter correctly.

This paper describes the techniques used to make laboratory measurements of the millimeter-wave opacity from gaseous ammonia under simulated Jovian conditions. The results of these experiments are applied to radiative transfer models which are used to compute the millimeter-wave emission from Jupiter. Other sources of millimeter-wave opacity in the Jovian atmospheres are also examined. New expressions for the microwave and millimeter- wave absorption from NH_3, H_2O, cloud condensates, and pressure-induced absorption from H_2, He and CH_4 are given and applied to the radiative transfer model. Reliable millimeter-wave observations are then compared to calculated emission spectra utilising expressions for the absorption from various atmospheric constituents based on recent laboratory studies.

2. Measurements of NH_3 Opacity at 3.2 mm

The absorption from gaseous ammonia (NH_3) in a simulated Jovian atmosphere has been measured at 7.5-9.38 mm (32-40 GHz) by Joiner *et al.* (1989). These measurements were compared to three theoretical formalisms. Although the data appeared to rule out the Van-Vleck Weiskopf (1945) lineshape, it was not clear whether the Gross (1955) lineshape or some modified form of the Ben-Reuven (1966) lineshape most accurately described the behavior of NH_3 at millimeter wavelengths. In order to further evaluate the millimeter-wave absorption from gaseous NH_3, we have made measurements of its opacity at a frequency of 94 GHz (3.2 mm) under simulated conditions for the Jovian planets. At this frequency the lineshapes differ by a significant amount, thus allowing a more accurate determination of the absorbing properties of ammonia at the high frequency tail of its pressure-broadened inversion spectrum. These experiments represent the first time that the opacity of gaseous NH_3 at wavelengths shortward of 7.5 mm has been measured under simulated conditions for the Jovian atmospheres.

Laboratory Configuration

The laboratory measurements are conducted using the W-Band millimeter-wave planetary atmospheres simulator shown in Figure 1. The W-Band millimeter-wave source consists of a power supply and backward wave oscillator (BWO) tube which act together as a millimeter-wave sweep oscillator. The millimeter-wave oscillator sweeps over the entire frequency range affected by the resonance in the Fabry-Perot resonator. The resonator is located inside a temperature chamber (ultra-low temperature freezer). Rigid pieces of WR-10 waveguide connect the resonator to the millimeter-wave source and receiver located outside the temperature chamber. The receiver utilises a harmonic mixer in which the local oscillator (LO) is a microwave source which is phased locked to a microwave frequency counter. The frequency of the LO is approximately 9.25 GHz. The tenth harmonic of the LO is then mixed with the outgoing signal from the resonator producing an intermediate frequency (IF) of about 1.5 GHz. The IF signal is coupled from the mixer to the high resolution spectrum analyzer. The spectral response of the resonator is then viewed with the high resolution spectrum analyzer.

The W-band Fabry-Perot resonator shown in Figure 2 consists of two gold plated mirrors, one flat and one spherical, which in effect produce a bandpass filter at the resonance. Electromagnetic energy is coupled both to and from the resonator through twin irises located on the flat mirror. The flat and curved mirrors have diameters of 5 and 11.5 cm respectively. The separation between the two mirrors is approximately 15 cm. This type of configuration yields superior focusing which is evident in the high quality factor (Q) of the resonator which is on the order of 25000.

The W-band resonator is contained in a cross shaped glass pipe with the curved mirror resting on two fixed support arms. The fixed arms can be adjusted in order to change the distance between the mirrors without disturbing the sensitive alignment of the mirrors. Each of the open ends of the pipe is sealed with an O-ring sandwiched between the glass lip and a flat brass or aluminum plate which is bolted to an inner flange. One of the plates contains an inlet for the gas to be introduced and evacuated. A network of 3/8" stainless steel tubing and valves connects the resonator to cylinders containing the various gases used in the experiments (H_2,

He, and custom mixture). In addition, the pipes are also connected to an oil diffusion vacuum pump, a thermocouple vacuum gauge tube (0-27 Torr), and a positive pressure gauge (0-100 PSIG). Each component may be isolated from the system using the valve configuration shown in Figure 1. The system is capable of containing two atmospheres of pressure without detectable leakage. The experiment takes place indoors with the gases being released outdoors through a vent pipe where they are safely diluted by air. A flammable gas detector is used to detect any leaks that may occur during the experiment.

Experimental Approach

The absorption from gaseous ammonia can be calculated by observing changes in the bandwidth and center frequency of a resonance with and without the absorbing gas present. For a low- loss gas such as NH_3, if the percentage change in the center frequency of the resonance with and without the NH_3 present is small (for our experiment, the percentage change is approximately 0.3%), then the absorptivity can be expressed as

$$\alpha \simeq (BW_L - BW_C)\frac{2\pi}{c} = 2.096 \cdot 10^{-4}(\Delta BW) \ \ cm^{-1} \quad (2.2)$$

where ΔBW is the change in bandwidth (in MHz) of the resonance with and without the absorbing gas present.

In order to evaluate Equation 2.2, the loaded bandwidth of the 94 GHz resonance, BW_L, is first measured while the gas chamber is filled with a premixed $H_2/He/NH_3$ mixture. The quantity BW_C is found by measuring the bandwidth in an H_2/He mixture (no NH_3 present) instead of using the bandwidth measured in an evacuated chamber. This approach accounts for the *dielectric loading* effect which is described at length in Joiner *et al.* (1989).

In order to observe the absorption due to ammonia with our system, a fairly high mixing ratio of NH_3 is needed. A premixed, constituent analyzed mixture (Matheson) consisting of 85.56% H_2, 9.37% He, and 5.07% NH_3 is used in all experiments. In order to avoid condensation, the experiments take place at a temperature of 210 K. The pressures of the experiments range from 1 to 2 atm.

Experimental Uncertainties

The main contribution to the uncertainty in this type of measurement is due to noise in the system. This noise is visible when measuring the bandwidth of a resonance with the spectrum analyzer. The uncertainty in measured absorptivity due to noise in our system is on the order of ± 20-25%. Other uncertainties are due to instrumental error and include the uncertainty in the ammonia mixing ratio, uncertainty in the measurement of total pressure, and variations in the chamber's temperature. The combined uncertainties in the absorption coefficient resulting from these three sources is approximately ±5%. The total uncertainty from all sources is reflected in the reported error bars.

The uncertainty in the measurement of center frequency and bandwidth (disregarding noise) is affected by the microwave LO source as well as the spectrum analyzer. By phase locking the microwave LO source to a microwave frequency counter and properly calibrating the spectrum analyzer, these uncertainties become negligible.

Experimental Results

Several different theories have been used to describe the frequency dependent part of the collision or pressure broadening of NH_3 inversion lines broadened in a H_2/He atmosphere. The Van Vleck-Weisskopf (1945) lineshape is known to be accurate at low pressures (less than 1 atm). Zhevakin and Naumov (1963) derived a different lineshape and found that their lineshape gave better results than the Van Vleck-Weisskopf theory when applied to experimental data regarding atmospheric water vapor absorption. This lineshape was also derived independently by Gross (1955). It is sometimes referred to as the kinetic lineshape. The formalisms for computing these lineshapes are given in Joiner *et al.* (1989). Ben-Reuven (1966) derived a more comprehensive lineshape which was found to be more accurate at higher pressures. This lineshape can be shown to reduce to the other lineshapes under certain conditions. The parameters of this lineshape may be varied in order to be compatible with laboratory measurements as in Berge and Gulkis (1976) and as we have done below. Figure 3 shows a graph of the calculated absorption from ammonia based upon four of the theoretical formalisms described above. The center frequencies and self-broadened linewidths (γ_o) of the NH_3 inversion resonances used in all calculations are taken from Poynter and Kakar (1975). The submillimeter lines are calculated as in dePater and Massie (1985) except that the Gross lineshape is used instead of the Van Vleck- Weisskopf lineshape.

The results of the measurements of NH_3 absorption at 3.2 mm are given in Table 1 along with the theoretically-derived values using various formalisms. It is clear that neither the Van Vleck-Weisskopf nor the Gross lineshapes provides a good fit to these measurements. We have modified the parameters of the Ben- Reuven lineshape in order to be compatible with the results of this work as well as the work of Morris and Parsons (1970), Steffes and Jenkins (1988), Joiner *et al.* (1989) and Spilker (1990). This formalism employs the Ben-Reuven lineshape as described in Berge and Gulkis (1976) with the pressure-broadened linewidth and coupling element given by

Table 1

$$\gamma(j,k) = 1.69P_{H_2}\left(\frac{300}{T}\right)^{2/3} + 0.75P_{He}\left(\frac{300}{T}\right)^{2/3}$$

$$+0.6P_{NH_3}\left(\frac{300}{T}\right)\gamma_o(j,k) \ \ GHz \quad (2.3)$$

$$\varsigma(j,k) = 1.35P_{H_2}\left(\frac{300}{T}\right)^{2/3} + 0.3P_{He}\left(\frac{300}{T}\right)^{2/3}$$

$$+0.2P_{NH_3}\left(\frac{300}{T}\right)\gamma_o(j,k). \ \ GHz \quad (2.4)$$

No additional correction term is used in this formalism.

3. Application of Results to Radiative Transfer Model

A forward modeling approach is taken in which the parameters of the radiative transfer model are varied in an attempt to fit the calculated emission spectra to radio astronomical observations. The disk-average brightness of a planet, at a frequency ν is given by

$$B_\nu(T_D) = 2\int_0^1 \int_0^\infty B_\nu(T) exp\left(-\frac{\tau}{\mu}\right) d\tau \ d\mu. \quad (3.1)$$

where $B_\nu(T)$ is the Planck function The quantity μ is the cosine of the zenith angle. The zenith angle at a given point on a constant pressure surface in the atmosphere of the planet is defined as the angle between the line of sight to the planet and the local normal to the surface at that point. The optical depth, τ, is defined as

$$\tau_\nu(z) = \int_0^z \alpha_\nu(z)dz \qquad (3.2)$$

where z is the depth as measured from the top of the planet and $\alpha_\nu(z)$ is the sum of all the absorbing processes at a frequency ν. The pressure may be related to depth in the atmosphere by the hydrostatic equation and the equation of state.

The integral in Equation 3.1 is evaluated downward from the top of the atmosphere ($z = 0$) and is terminated when a value of 5 optical depths for τ is reached. We have evaluated the integral over μ in Equation 3.1 for Jupiter using two methods. The first method takes into account the oblate shape of the planet by using a grid approach (*e.g.* dePater and Massie, 1984). The second method assumes a spherical shape for the planet. Since the two methods differed by less than 1K or about 0.05%, we use the spherical approximation for all model calculations.

Temperature-Pressure Profile

The temperature-pressure profile, T(P), is calculated as in Briggs and Sackett (1989). A saturated adiabatic lapse rate is used as the calculation of T(P) evolves from deep in the atmosphere. The parameters for latent heat release are taken from Briggs and Sackett (1989). The *intermediate* case for the specific heat of hydrogen (Wallace, 1980) is assumed. The T(P) profile is calculated iteratively and constrained to meet the 1 bar temperature of 165K derived from the *Voyager* radio occultation experiments (Lindal *et al.*, 1981). At pressures from 10 mbar to 1 bar, a T(P) profile derived from *Voyager* data is used, which corresponds to the whole Jovian disk (similar to Bezard *et al.*, 1983). The T(P) profile is shown in Figure 4.

Pressure-Induced Absorption

Pressure-induced absorption is caused by the transient dipole which is induced by intermolecular forces in colliding H_2-H_2, H_2-He, and H_2-CH_4 molecules. Goodman (1969) developed a simple expression for calculating the microwave and millimeter-wave pressure-induced absorption of H_2-H_2 and H_2-He pairs. We have updated this expression so that it is consistent with empirical expressions which have been used to describe more recent laboratory data taken at infrared wavelengths by Bachet *et al.* (1983) and Dore *et al.* (1983). New parameters for the temperature and pressure dependencies in the Goodman (1969) expression have been fit to a six parameter model from Borysow *et al.* (1985). A term which accounts for the H_2- CH_4 absorption has also been added. The parameters for this expression were optimized for temperatures and pressures corresponding to Jupiter's atmosphere. The new expression is

$$\alpha_{H_2} = \frac{3.56e-11}{\lambda^2} P_{H_2} \cdot \left[P_{H_2} \left(\frac{273}{T}\right)^{3.12} + 1.38 P_{He} \left(\frac{273}{T}\right)^{2.24} + 9.32 P_{CH_4} \left(\frac{273}{T}\right)^{3.84} \right] \ cm^{-1} \qquad (3.3)$$

where P_{H_2}, P_{He}, P_{CH_4} are the partial pressures of hydrogen, helium, and methane in bars and λ is the wavelength in cm. This expression deviates from the Borysow formalism by less than 1% for temperatures and pressures at altitudes above the 10 bar level in Jupiter's atmosphere. For the Jovian conditions in the 10 to 100 bar region, the new expression deviates from the Borysow formalism by less than 10%.

H_2O Absorption

We use an expression for water vapor absorption under Jovian conditions which is based on laboratory data under terrestrial conditions. The parameters for the water vapor lines (*i.e.* transition frequencies, line strengths, linewidths) are summarized in Ulaby *et al.* (1981) from a more detailed compilation given in Waters (1976). This calculation includes ten rotational lines with frequencies up to 448 GHz. The kinetic lineshape is used in this calculation along with a correction term which was empirically derived by Gaut and Reifenstein (1971). The term P appearing in the expressions given by Ulaby *et al.* (1981), representing the pressure under terrestrial conditions, is replaced by $(0.81P_{H_2} + 0.25P_{He})$ in order to take into account the broadening characteristics of the Jovian atmosphere.

H_2S Absorption

Several strong rotational lines of H_2S appear in the millimeter spectrum at frequencies near 168, 217 and 300 GHz. We use a model of hydrogen sulfide absorption which is based on line strengths and center frequencies given in the GEISA catalog. We estimate the nitrogen-broadened line width to be approximately 2 GHz/bar based on its broadening of NH_3 and H_2O. We use a pressure-broadened linewidth of $d\nu = 2 \cdot (0.81P_{H_2} + 0.25P_{He})\left(\frac{300}{T}\right)^{2/3}$ GHz/bar and the Gross lineshape.

Cloud Absorption

An expression for the absorption due to cloud condensates based on Rayleigh scattering has been integrated into our radiative transfer model. In the Rayleigh regime, the absorption is expressed by

$$\alpha = \frac{18\pi M}{\rho\lambda} \cdot \left[\frac{\epsilon''}{(\epsilon'+2)^2 + \epsilon''^2} \right] \ cm^{-1} \qquad (3.4)$$

(Battan, 1973) where ρ is the density of the condensation particle, M is the bulk density of the cloud in the same units, λ is the wavelength in cm, and $\hat{\epsilon} = \epsilon' - j\epsilon''$ is the complex dielectric constant of the cloud material (related to the complex index of refraction, $\hat{n} = n - jk$, by $\hat{\epsilon} = \hat{n}^2$).

Using Equation 3.4 along with models for cloud bulk densities based on equilibrium condensation models (see *e.g.* Briggs and Sackett, 1989), cloud opacity has been added to our Jovian model. The bulk densities calculated with equilibrium condensation models assume total condensation and thus the maximum expected bulk densities of cloud condensates. Romani (*private communication*, 1990) suggests that the actual cloud densities on Jupiter may be a factor of 5 lower than those predicted with equilibrium condensation models. Thus, the cloud bulk density will be taken as a

variable in the calculating the absorption from cloud condensates.

Previous models have included only the contribution from the NH_3 ice cloud. However, weighting functions show that most of the emission from Jupiter at millimeter wavelengths originates from pressures levels between 1 and 3 bars. Thus, the potential contributions from any NH_4SH cloud as well as from H_2O (ice and aqueous solution) clouds should also be included. Because the complex index of refraction of the condensates at these wavelengths is not known, values were extrapolated from laboratory measurements in the infrared by Sill *et al.* (1980). A values of 1.3 is used for n_{NH_3}, the real part, and values between 0.01 and 0.05 for k_{NH_3}, the imaginary part of the index of refraction are used in our model program. Similarly, a value of 1.7 (CRC) is used for n_{NH_4SH} and values between 0.01 and 0.05 are used for k_{NH_4SH}. Values of 1.78 for n_{H_2O} and 0.01 for k_{H_2O} (ice) are taken from Ulaby *et al.* (1981). An expression for absorption by liquid water is given in Briggs and Sacket (1989).

4. Discussion

We have surveyed the existing microwave and millimeter-wave observations of Jupiter and compiled a list of reliable observations to use as a basis for comparison with theoretically computed spectra of Jupiter. A list of reliable observations published at frequencies from 36 to 300 GHz (1-8.35 mm) is given in Table 2 along with corresponding calibration sources and spectral bandwidths. Klein and Gulkis (1978) have normalized all of the observations between 14.5 and 36 GHz (8.35-20.7 mm) to a common flux scale. At longer wavelengths, Berge and Gulkis (1976) have given a survey in which the observations have been based on a common flux scale whenever possible.

Vertical distributions of NH_3, H_2S and H_2O have been derived by assuming various sub-cloud mixing ratios for cloud-forming constituents and using equilibrium condensation models. The derived abundance profiles are then used in the radiative transfer model in order to predict the emission from Jupiter. Four distributions for NH_3, two for H_2S and one for H_2O are shown in Figure 4. Abundance profiles for NH_3 assume deep mixing ratios of $2.5 \cdot 10^{-4}$ and $3.0 \cdot 10^{-4}$ which correspond to the measured value and upper limit derived by Bjoracker *et al.* (1986a) at 5μm. Distributions for H_2S assume sub-cloud mixing ratios equal to the solar abundance ($3.55 \cdot 10^{-5}$) and nearly ten times the solar abundance ($2.2 \cdot 10^{-5}$) respectively. The H_2S is rapidly depleted due to a reaction with NH_3 to form NH_4SH. The H_2S distributions are compatible with the upper limits derived by Larson *et al.* (1984) at 2.7μm. For sub-cloud H_2S mixing ratios less than or equal to the solar abundance, the NH_3 mixing ratio is not significantly depleted (as in NH_3 distributions 1a and 1b). However, if the H_2S mixing ratio is increased to $2.2 \cdot 10^{-5}$ (as in distribution 2), NH_3 becomes depleted near 2 bars (as in NH_3 distributions 2a and 2b). The formation of an NH_3 ice cloud further depletes the ammonia near 0.75 bar. The H_2O distribution assumes a sub-cloud mixing ratio equal to the solar abundance ($1.23 \cdot 10^{-3}$) and is depleted by the formation of an ice and aqueous H_2O cloud.

The distributions and cloud bulk densities shown in Figure 4 may not represent the actual distributions in Jupiter's atmosphere, but are used as a basis to test the effects of the various absorbers on the computed Jovian spectrum. For example, the actual H_2O distribution in Jupiter's atmosphere may be depleted by a factor of 100 (Bjoracker *et al.*, 1986b). The H_2O distributions and bulk densities shown in Figure 4 are used to illustrate the maximum possible effect of H_2O (gas and clouds) on Jupiter's emission. Although actual distribution of gases within the belts and zones of the planets will vary from the those shown in Figure 4, the distributions we show represent values averaged over the disk of the planet and hence are used to calculate disk-averaged brightness temperatures.

In Figure 5, the observed Jovian spectrum is shown along with calculated emission spectra. The model calculations include only NH_3 and H_2O opacity and use the four NH_3 distributions shown in Figure 4. The error bars for observations using Mars as the primary calibrator include a 10% uncertainty for the calibration in addition to the systematic uncertainties reported in Table 2. Model calculations using all four NH_3 distributions provide a good fit to observations near 1.3 cm and at longer wavelengths. However, only NH_3 distributions 1a and 1b provide a good fit to the millimeter-wave observations. The influence of the 183 GHz H_2O line on the computed emission is small for NH_3 distributions 1a and 1b.

The effect of adding H_2S opacity to model Jovian emission for two NH_3 distributions is shown in Figure 6 (solid line: NH_3 and H_2S opacity only, dashed line: NH_3, H_2O and H_2S opacity). In order to account for the large bandwidths of many of the observations, the contribution from the H_2S lines are averaged over 70 GHz. The average contribution (dotted line) from H_2S is small for NH_3 distribution 1b but substantial for NH_3 distribution 2a. Bezard *et al.* (1983) have shown the potential effects of H_2S on Jupiter's emission for distributions in which the H_2S is not depleted by an NH_4SH cloud.

Figure 7 shows calculated emission spectra with and without cloud opacity included using NH_3 distribution 2b. Substantial opacity is provided by the clouds when values of 0.05 are used for k_{NH_3} and k_{NH_4SH} and the maximum cloud bulk densities from equilibrium condensation models are used. This case corresponds to the maximum possible effect of the absorption from clouds. However, when values of 0.01 for k_{NH_3} and k_{NH_4SH} are used and the cloud bulk densities decreased by a factor of 5, corresponding to a more realistic scenario, the opacity provided by the clouds becomes negligible.

5. Conclusions and Suggestions for Future Work

Using our new formalism for the Ben-Reuven lineshape in model calculations, we find that the millimeter-wave observations of Jupiter *can* adequately be explained using NH_3 opacity alone. Good fits to the observed spectrum are achieved using vertical distributions for NH_3 derived from equilibrium condensations models with deep mixing ratios of $2.5 - 3 \cdot 10^{-4}$ (solar abundance enhanced by a factor of 1.7-2) for NH_3 and less than or equal to the solar abundance ($3.35 \cdot 10^{-4}$ for H_2S.

Gaseous hydrogen sulfide may be providing additional opacity. Observations with greater spectral resolution are needed in order to detect the potential dips in emission due to H_2S and thus distinguish the effects of H_2S opacity from those of NH_3. Absorption by cloud condensates may also be providing opacity. However, due to large uncertainties in

the dielectric properties of the condensates and cloud bulk densities, no firm conclusions regarding cloud opacities can be drawn at this time.

More laboratory measurements are needed in order to further evaluate the millimeter-wave and microwave properties of the outer planets. We plan to make measurements of the hydrogen and helium pressure-broadened linewidths of millimeter-wave lines of gaseous hydrogen sulfide in the future. In addition, measurements of the dielectric properties of solid NH_3 and NH_4SH are also needed to accurately assess the effect of cloud condensates on the millimeter-wave spectra of the outer planets.

Acknowledgements. The authors thank Drs. D. P. Campbell, J. J. Gallagher and S. Halpbern of the Georgia Tech Research Institute (GTRI) and T.E. Brewer (Georgia Tech) for their generous assistance with the laboratory equipment and for providing illuminating discussions in this area. We also thank Drs. T. R. Spilker (Stanford), I. dePater (Berkeley), P. Romani (NASA-Goddard, SSAI), K. S. Noll (NASA-Marshall), B. Bezard and E. Lellouch (Observatoire de Paris- Meudon) for illuminating discussions.

This work was supported by the Planetary Atmospheres Program of the Solar System Exploration Division (Office of Space Science and Applications) of the National Aeronautics and Space Administration under Grant NAGW-533 and by the Georgia Tech Space Grant Consortium.

References

Bachet, G., E. R. Cohen, P. Dore, and G. Birnbaum 1983. The translational-rotational absorption spectrum of hydrogen. *Can. J. Phys* 61, 591-603.

Battan, L. J. 1973. *Radar Observation of the Atmosphere.* University of Chicago Press, Chicago.

Ben-Reuven, A. 1966. Impact broadening of microwave spectra. *Phys. Rev.* 145, 7-22.

Berge, G. L., and S. Gulkis 1976. Earth-based radio observation of Jupiter: Millimeter to meter wavelengths. In *Jupiter* (T. Gehrels, Ed.), 621-692. Univ. of Arizona Press, Tuscon.

Bezard, B., A. Marten, J. P. Baluteau, D. Gautier, J. M. Flaud, and C. Camy-Peyret 1983. On the detectability of H_2S in Jupiter. *Icarus* 55, 259-271.

Bjoracker, G. L., H. P.Larson, and V. G. Kunde 1986a. The gas composition of Jupiter derived from 5μm airborne spectroscopic observations. *Icarus* 66, 579-609.

Bjoracker, G. L., H. P.Larson, and V. G. Kunde 1986b. The abundance and distribution of water vapor in Jupiter's atmosphere *Astrophys. J.* 311, 1058-1072.

Borysow, J., L. Trafton, and L. Frommhold 1985. Modeling of Pressure-Induced Far-Infrared Absorption Spectra: Molecular Hydrogen Pairs. *Astrophys. J.* 296, 644-654.

Briggs, F. H., and P. D. Sackett 1989. Radio observations of Saturn as a probe of its atmosphere and cloud structure. *Icarus* 80, 77-103.

CRC Press 1980. *CRC Handbook of Chemistry and Physics* (R. C. Weast, Ed.). CRC Press, Boca Raton, FL.

Courtin, R., N. Coron, T. Encrenaz, R. Gispert, P. Bruston, J. Leblanc, G. Dambier, A. Vidal-Madjar 1977. Observations of giant planets at 1.4 mm and consequences on the effective temperatures. *Astron. and Astrophys.* 60, 115-123.

de Pater, I., and S. T. Massie 1985. Models of the millimeter-centimeter spectra of the giant planets. *Icarus* 62, 143-171.

Dore, P., L. Nencini, and G. Birnbaum 1983. Far infrared absorption in normal $H_2$from 77 to 298K. *J. Quant. Spec. Rad. Trans* 30, 245-253.

Gaut N. E. and E. C. Reifenstein III 1971. Environmental Research and Technology, Inc., Report No. 13, Lexington, MA.

Goodman, G. C. 1969. Models of Jupiter's atmosphere *Ph. D. thesis* , University of Illinois, Urbana.

Griffin, M. J., P. A. R. Ade, G. S. Orton, E. I. Robson, W. K. Gear, I. G. Nolt, and J. V. Radostitz 1986. Submillimeter and millimeter observations of Jupiter. *Icarus* 65, 244-256.

Gross, E. P. 1955. Shape of collision-broadened spectral lines. *Phys. Rev.* 97, 395-403.

Joiner, J., P. G. Steffes, and J. M. Jenkins 1989. Laboratory measurements of the 7.5-9.38 mm absorption of gaseous ammonia (NH_3) under simulated Jovian conditions. *Icarus* 81, 386-395.

Klein, M. J. and S. Gulkis 1978. Jupiter's atmosphere: Observations and interpretation of the microwave spectrum near 1.25 cm wavelength. *Icarus* 25, 44-60.

Larson, H. P., D. S. Davis, R. Hofman, and G. L. Bjoraker 1984. The Jovian atmospheric window at 2.7 microns: A search for H_2S. *Icarus* 60, 621-639.

Lindal, G. F., G. E. Wood, G. S. Levy, J. O. Anderson, D. N. Sweetnam, H. B. Hotz, B. J. Buckles, D. P. Holmes, P. E. Dams, V. R. Eshleman, G. L. Tyler, and T. A. Croft 1981. The atmosphere of Jupiter: An analysis of the Voyager Radio Occultation measurements. *J. Geophys. Res.* 86, 8721-8727.

Morris, E. C., and R. W. Parsons 1970. Microwave absorption by gas mixtures at pressures up to several hundred bars. *Astron. J. Phys.* 23, 335-349.

Poynter, R. L., and R. K. Kakar 1975. The microwave frequencies, line parameters, and spectral constants for NH_3. *Astrophys. J. Suppl.* 29, 87-96.

Sill, G., U. Fink, and J. R. Ferraro 1980. Absorption coefficients of solid NH_3 from 50-7000 cm^{-1}. *J. Opt. Soc. Am.* 70, 724-739.

Spilker, T. R. 1990. Laboratory measurements of Microwave absorptivity and refractivity spectra of gas mixtures applicable to giant planet atmospheres. *Ph. D. thesis* , Stanford University, Stanford.

Ulaby, F. T., R. K. Moore, A. K. Fung 1981. *Microwave Remote Sensing Active and Passive.* Addison-Wesley Publishing Company, Inc. Reading, MA.

Ulich, B. L. 1974. Absolute brightness temperature measurements at 2.1 mm wavelength. *Icarus* 21, 254-261.

Ulich, B. L. 1981. Millimeter-wavelength continuum calibration sources. *Astron. J.* 86, 1619-1626.

Ulich, B. L., J. R. Cogdell, and J. H. Davis 1973. Planetary brightness temperature measurements at 8.6mm and 3.1 mm wavelengths. *Icarus* 19, 59-82.

Ulich, B. L., J. H. Davis, P. J. Rhodes, and J. M. Hollis 1980. Absolute brightness temperature measurements at 3.5 mm wavelength. *IEEE Trans. Ant. Prop.*, AP-28, No. 3, 367-377.

Ulich, B. L., J. R. Dickel, and I. dePater 1984. Planetary Observations at a wavelength of 1.32 mm. *Icarus* 60, 590-598.

Van Vleck, J. H., and V. F. Weisskopf 1945. On the shape of collision-broadened lines. *Rev. Mod. Phys.* 17, 433-443.

Wallace, L. 1980. The structure of the Uranus atmosphere. *Icarus* 43, 231-259.

Waters, J. W. 1976 Absorption and emission of microwave radiation by atmospheric gases. In *Methods of Experimental Physics*, M. L. Meeks , ed.,12 Part B, Radio Astronomy, Academic Press, Section 2.3.

Werner M. W., G. Neugebauer, J. R. Houck, and M. G. Hauser 1978. One millimeter brightness temperatures of the planets. *Icarus* 35, 289-296.

Zhevakin, S. A., and A. P. Naumov 1963. Coefficient of absorption of electromagnetic waves by water vapor in the range 10 microns-2 cm. *Radiophys. Quantum Electron.* 6, 674-694.

J. Joiner and P. G. Steffes, Georgia Institute of Technology, School of Electrical Engineering, Atlanta, GA 30332-0250

(Received February 15, 1991;
revised ;
accepted ;)

Paper number .

JOINER AND STEFFES: JUPITER'S MILLIMETER-WAVE SPECTRUM
JOINER AND STEFFES: JUPITER'S MILLIMETER-WAVE SPECTRUM
JOINER AND STEFFES: JUPITER'S MILLIMETER-WAVE SPECTRUM
JOINER AND STEFFES: JUPITER'S MILLIMETER-WAVE SPECTRUM
JOINER AND STEFFES: JUPITER'S MILLIMETER-WAVE SPECTRUM
JOINER AND STEFFES: JUPITER'S MILLIMETER-WAVE SPECTRUM

Fig. 1. Block diagram of the planetary atmospheres simulator as configured for the measurement of millimeter-wave NH_3 absorption under simulated Jovian conditions.

Fig. 2. Sketch of the Fabry-Perot resonator which operates at 94 GHz (3.2 mm).

Fig. 3. Theoretically derived absorption profiles in a 90% H_2-10% He-0.03% NH_3 mixture at 2 bars and 200K using the Van Vleck Weisskopf lineshape (VVW, dot-dashed line), Zhevakin-Naumov or Gross lineshape (ZN-G, dotted line), Ben-Reuven lineshape as per Berge and Gulkis (BR-BG, dashed line) and Ben-Reuven formalism as given in this paper (BR-JS, solid line).

Fig. 4. Various abundance profiles for NH_3 and H_2S and cloud bulk densities based on equilibrium condesation models. Model 1:$\chi_{H_2S} = 3.35 \cdot 10^{-5}$ (solar), 2a: $\chi_{NH_3} = 2.5 \cdot 10^{-4}$, 2b: $\chi_{NH_3} = 3 \cdot 10^{-4}$; Model 2:$\chi_{H_2S} = 2.2 \cdot 10^{-4}$, 1a: $\chi_{NH_3} = 2.5 \cdot 10^{-4}$, 1b: $\chi_{NH_3} = 3 \cdot 10^{-4}$; $\chi_{H_2O} = 1.23 \cdot 10^{-3}$ (solar). Temperature-Pressure profile calculated with $\chi_{NH_3} = 2.5 \cdot 10^{-4}, \chi_{H_2S} = 3.3 \cdot 10^{-5}, \chi_{H_2O} = 1.0 \cdot 10^{-5}$

Fig. 5. Observed Jovian spectrum (error bars include 10% uncertainty for observations using Mars as calibrator) and computed emission using NH_3 and H_2O opacity only and vertical distributions in Figure 4.

Fig. 6. Observed Jovian spectrum with computed emission using NH_3 distributions 1b and 2a with H_2S distributions 1 and 2 respectively from Figure 4. Dashed line: NH_3 and H_2O opacity only; Solid line: NH_3, H_2O and H_2S opacity; Dotted line NH_3, H_2O and H_2S opacity averaged over a bandwidth of 70 GHz.

Fig. 7. Observed Jovian spectrum with computed emission using NH_3 profile 2b with and without cloud opacity included. Solid line: NH_3 and H_2O opacity only; Dashed line: $k_{NH_3}, k_{NH_4SH} = 0.05$ and maximum bulk densities as shown in Figure 4 (Dotted line below: H_2S opacity added); Dot-dashed line: $k_{NH_3}, k_{NH_4SH} = 0.01$ and maximum bulk densities (same result obtained for $k_{NH_3}, k_{NH_4SH} = 0.05$ and densities decreased by a factor of 5); Dotted line above: $k_{NH_3}, k_{NH_4SH} = 0.01$ and bulk densities decreased by a factor of 5

TABLE I: Absorption summary for NH_3 at 3.2 mm
85.56%H_2, 9.37%He, 5.07%NH_3, T=210K

Date	Press. (atm)	α meas. (dB/km)	α ZN/G	α VVW	α BR-BG	α BR-JS
10/20/88	2.0	115±32	42.3	350.6	117.0	120.8
	2.0	109±32	42.3	350.6	117.0	120.8
	1.7	58±30	30.8	253.9	84.7	87.4
		36±30	30.8	253.9	84.7	87.4
	1.3	0±30	18.2	148.9	49.7	51.1
	1.0	0±30	10.8	88.3	29.4	30.3
10/22/88	2.0	91±30	42.3	350.6	117.0	120.8
10/22/88	2.0	91±30	42.3	350.6	117.0	120.8

TABLE 2. Millimeter-wave observations of Jupiter

λ (mm)	ν (GHz)	T_B (K)	Cal	$\Delta\nu$ (GHz)	Reference
1.0	300	168±8	Mars	102,229	Werner *et al.* (1978)
1.08	279	169.9±5.1	Mars	75	Griffin *et al.* (1986)
1.32	227	170.9±3.9	Mars	70	Griffin *et al.* (1986)
1.32	227	165±8	planets	39	Ulich *et al.* (1984)
1.4	214	[a]148±16	planets	275	Rather *et al.* (1975)
1.40	214	[b]168±11	Mars	210	Courtin *et al.* (1977)
2.00	150	173.3±1.1	Mars	50	Griffin *et al.* (1986)
2.13	141	[a]167±12	abs	1-2	Ulich (1974, 1981)
2.14	140	[a]178±13	abs	1-2	Cogdell *et al.* (1975)
3.09	97	[a]174±10	abs	0.1-0.2	Ulich *et al.* (1973)
3.33	90	172.5±1.4	Mars	1-2	Griffin *et al.* (1986)
3.48	86	179.4±4.7	abs	0.03-0.5	Ulich *et al.* (1980)
3.53	85	[a]166±6	DR21	1-2	Ulich (1974)

[a]Brightness temperatures as given in Berge and Gulkis (1976)

[b]Recalculated with beam correction factor in Ulich *et al.* (1980)

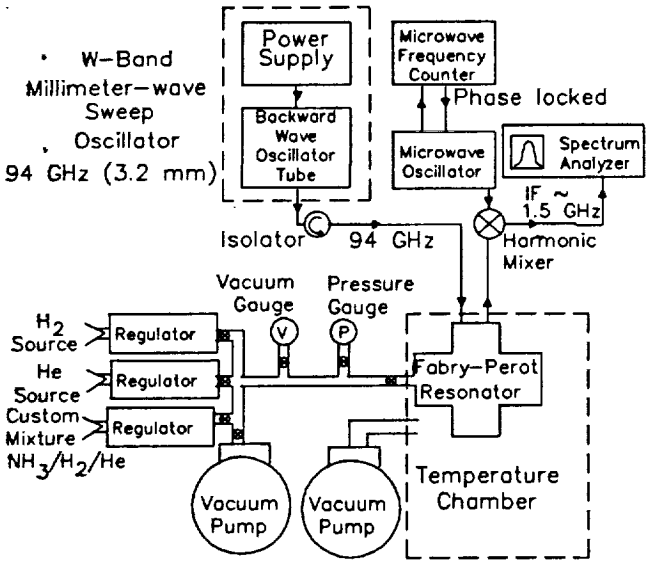
W-Band
Millimeter-wave
Sweep
Oscillator
94 GHz (3.2 mm)
Power Supply
Backward Wave Oscillator Tube
Microwave Frequency Counter
Phase locked
Microwave Oscillator
Spectrum Analyzer
IF ~ 1.5 GHz
Isolator
94 GHz
Harmonic Mixer
Vacuum Gauge
Pressure Gauge
V
P
H2 Source
He Source
Custom Mixture NH3/H2/He
Regulator
Regulator
Regulator
Fabry-Perot Resonator
Temperature Chamber
Vacuum Pump
Vacuum Pump

Figure 1

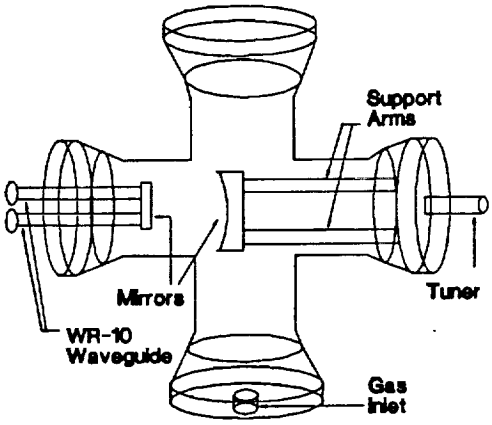

Figure 2

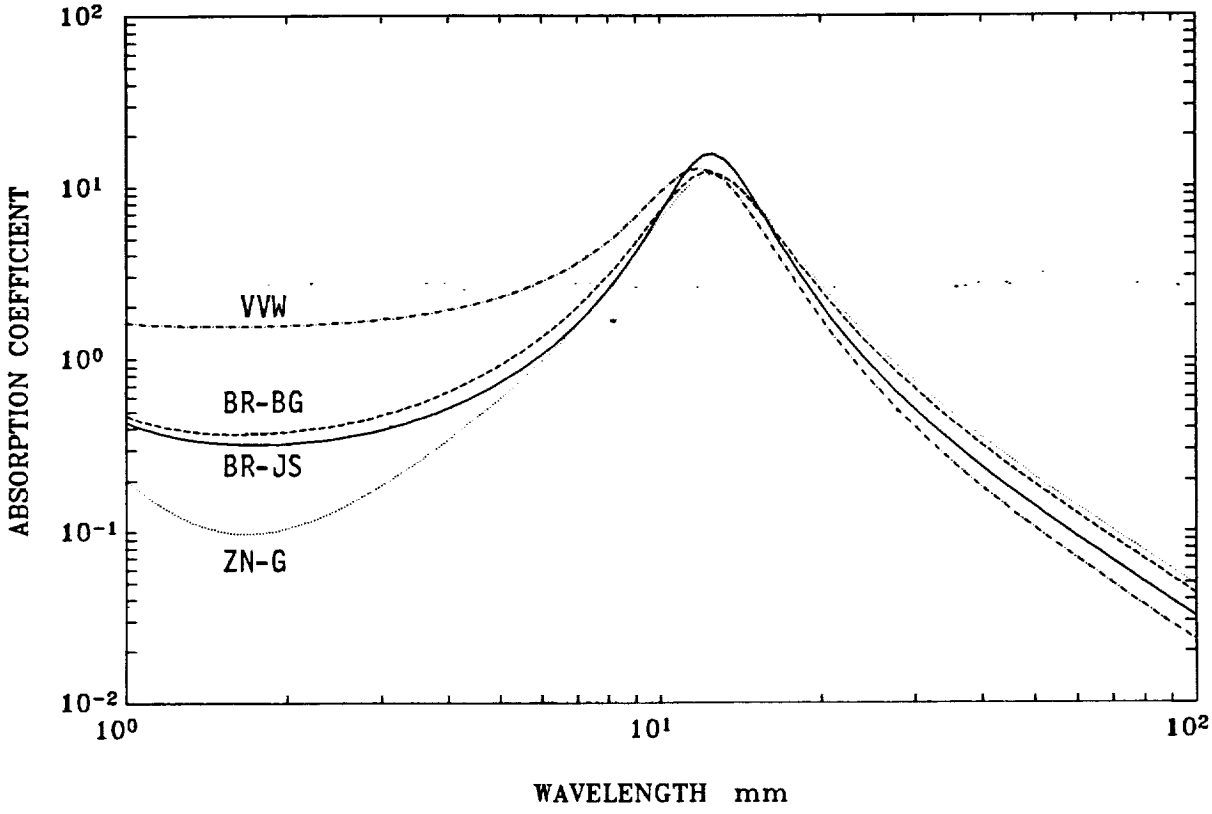
ABSORPTION COEFFICIENT
10^2
10^1
10^0
10^{-1}
10^{-2}
VVW
BR-BG
BR-JS
ZN-G
10^0
10^1
10^2
WAVELENGTH mm

Figure 3

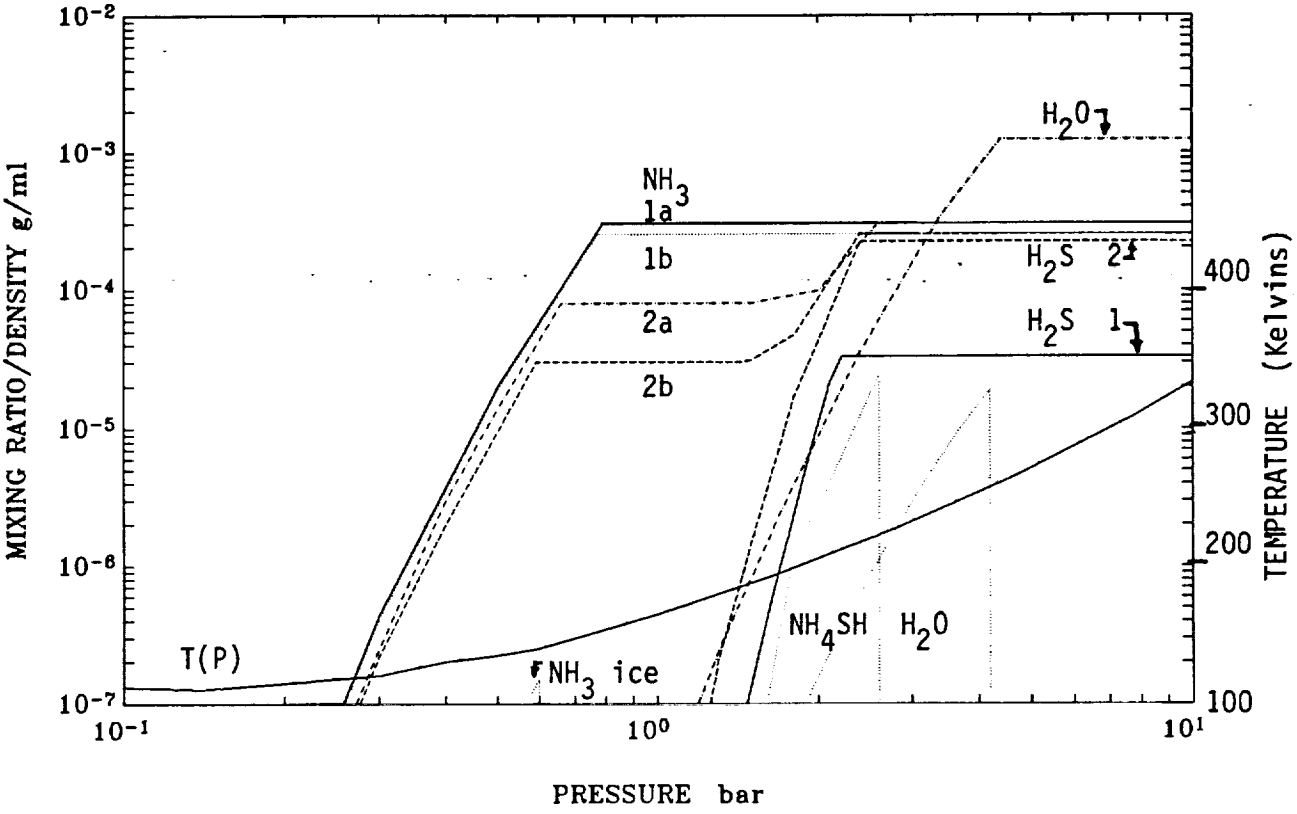
MIXING RATIO/DENSITY g/ml
TEMPERATURE (Kelvins)
PRESSURE bar
10^{-2}
10^{-3}
10^{-4}
10^{-5}
10^{-6}
10^{-7}
10^{-1}
10^{0}
10^{1}
100
200
300
400
H_2O
NH_3 1a
1b
2a
2b
H_2S 2
H_2S 1
T(P)
NH_3 ice
NH_4SH
H_2O

Figure 4

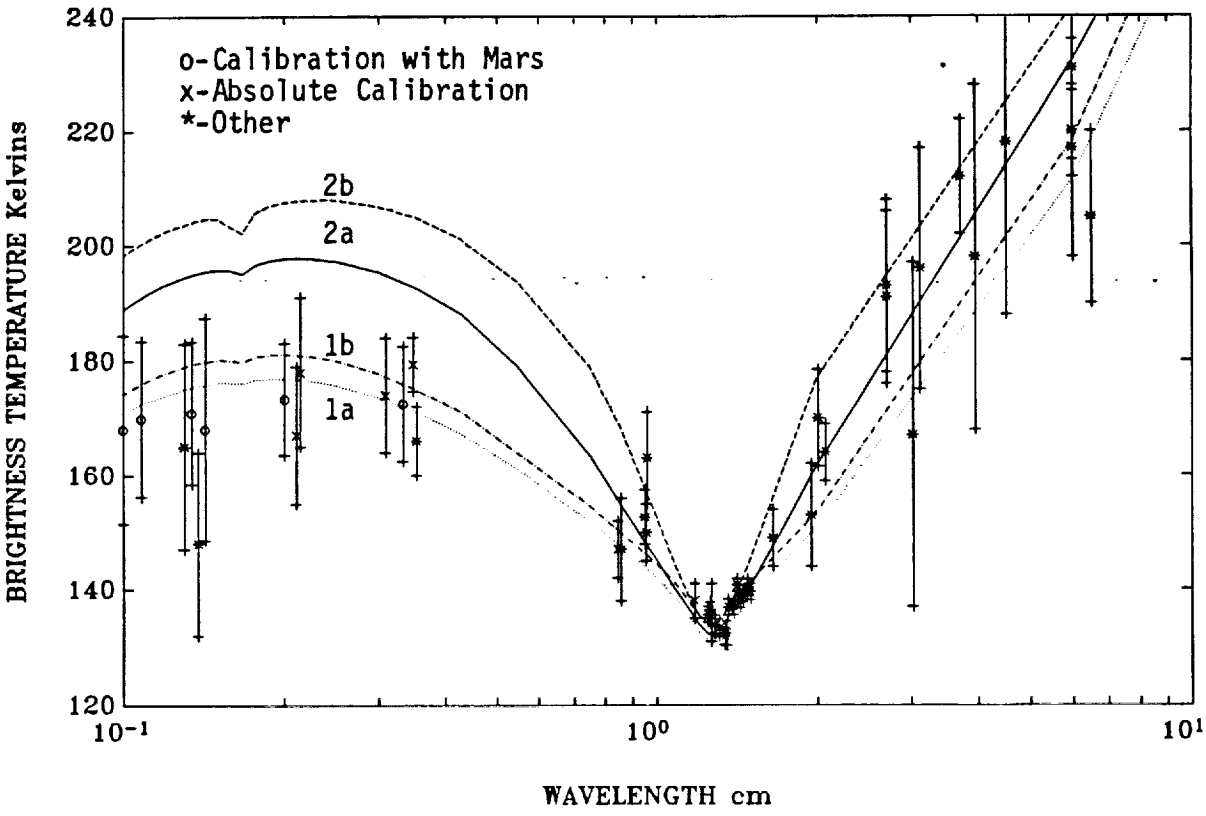
o-Calibration with Mars
x-Absolute Calibration
*-Other
2b
2a
1b
1a
240
220
200
180
160
140
120
10^{-1}
10^{0}
10^{1}
BRIGHTNESS TEMPERATURE Kelvins
WAVELENGTH cm

Figure 5

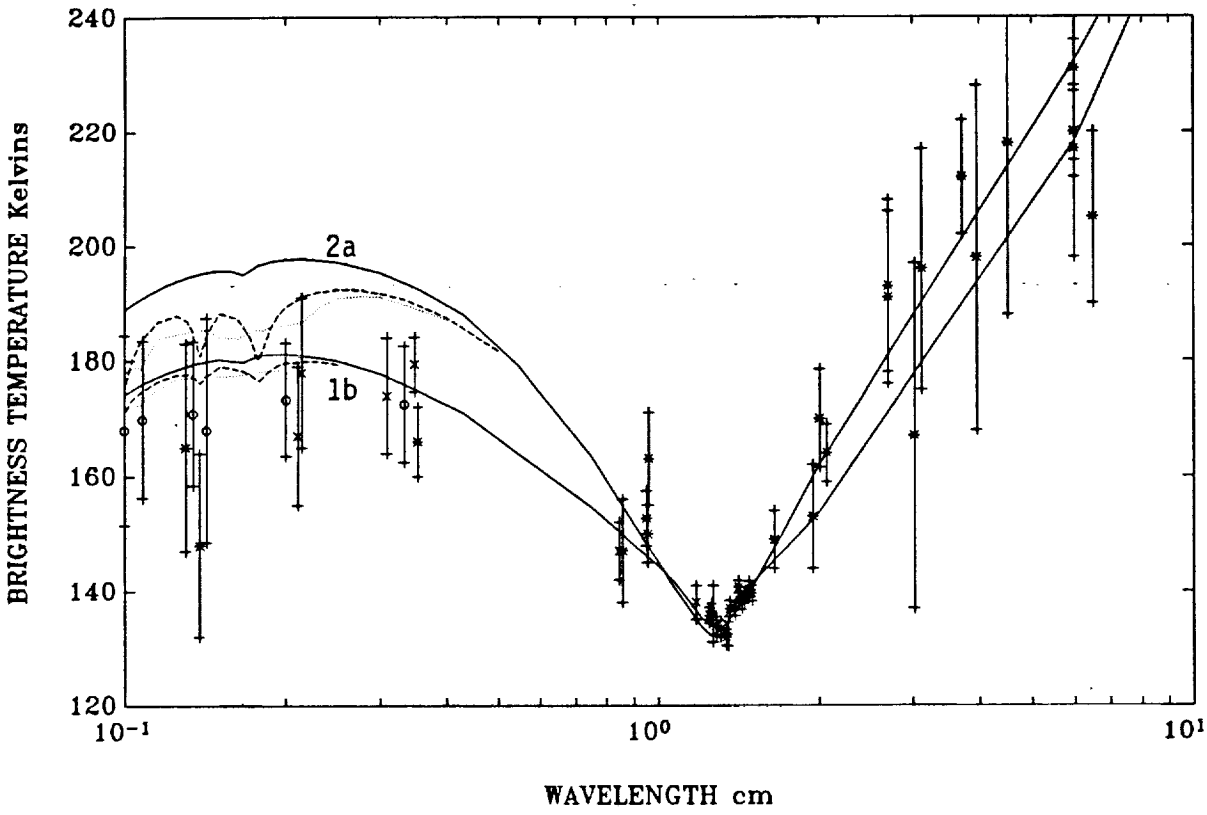
240
220
200
180
160
140
120
BRIGHTNESS TEMPERATURE Kelvins
2a
1b
10^{-1}
10^{0}
10^{1}
WAVELENGTH cm

Figure 6

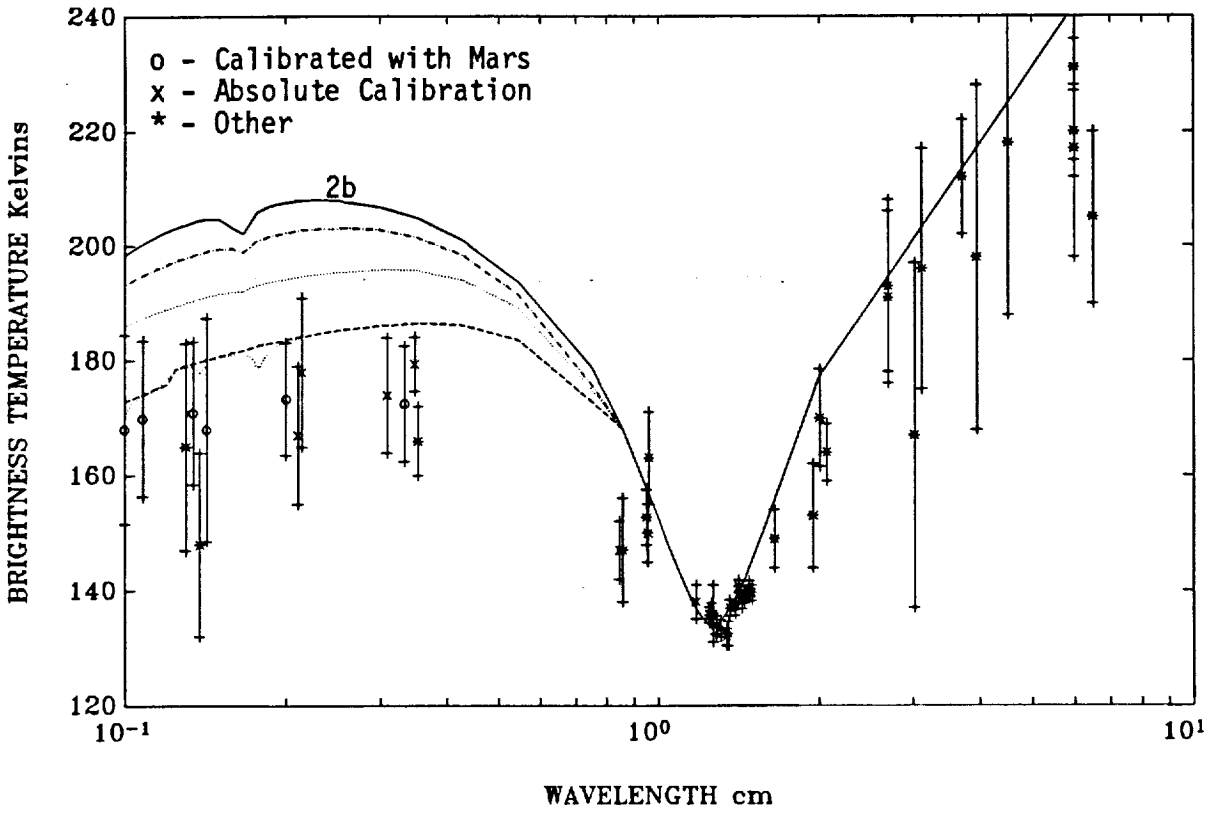
o - Calibrated with Mars
x - Absolute Calibration
* - Other
2b
240
220
200
180
160
140
120
BRIGHTNESS TEMPERATURE Kelvins
10^{-1}
10^{0}
10^{1}
WAVELENGTH cm

Figure 7

LABORATORY MEASUREMENT OF THE MILLIMETER-WAVE PROPERTIES OF LIQUID SULFURIC ACID (H_2SO_4).

Antoine K. Fahd and Paul G. Steffes

School of Electrical Engineering

Georgia Institute of Technology, Atlanta GA., 30332-0250

Abstract. Recent observations of the millimeter-wave (2.6 mm) emission from Venus have shown significant variations in its continuum flux emission (de Pater et al., 1991). Some of this change in emission may be attributed to variability in the abundance of Venus cloud constituents; specifically H_2SO_4 condensates. The ability to judge the validity of this assumption requires knowledge of the electrical properties of the absorbing condensate at millimeter-wave frequencies (30<f<300 GHz). In order to accurately model the effect of the condensates on the flux emission from Venus, a determination of the dielectric properties of liquid H_2SO_4 is essential. As a result, laboratory measurements of the complex dielectric constant of liquid sulfuric acid between 30-40 and 90-100 GHz have been performed.

The methodology and the results are reported in this paper along with a calculation of the absorption of H_2SO_4 droplets under Venus-like conditions. In addition, this paper discusses the effects of these condensates on the variation in the flux-emission of Venus and compares the effect of H_2SO_4 droplets with other absorbers in the atmosphere of Venus such as gaseous SO_2. We conclude that this condensate does affect the brightness temperature of Venus and its effect cannot be omitted in future modeling of the atmosphere of Venus.

I. Introduction

Recent observations of the millimeter-wave emission of Venus at 112 GHz (2.6 mm) have shown a 30 K variation in the observed flux emission as reported by de Pater et al. (1991). These emission variations may be attributed to variations in the abundance of absorbing constituents present in the middle atmosphere of Venus. Such constituents include gaseous H_2SO_4, SO_2, CO_2 and liquid sulfuric acid in the form of cloud condensate. (Detailed description regarding the presence of these constituents may be found in Steffes and Eshleman (1982), Steffes (1985), and Steffes et al. (1990)) Among these constituents, gaseous CO_2 is considered to be the primary absorber in the atmosphere of Venus. However, the CO_2 abundance variability is considered to be low and therefore cannot account for the measured variability in emission.

Recently, de Pater et al. (1991) suggested that this variability may be attributed to the variation in the abundance of the cloud condensate (i.e, liquid sulfuric acid). In order to evaluate this hypothesis, a knowledge of the dielectric properties of liquid sulfuric acid at millimeter-wave frequencies is needed so as to determine the expected absorptivity from such condensate, and hence the effect of this condensate on the emission spectrum of Venus. Estimation of the absorption of this condensate at millimeter-wave frequencies is not straightforward since no laboratory measurements of the dielectric constant of liquid H_2SO_4 have been previously reported at millimeter wavelengths. Although the dielectric properties of liquid H_2SO_4 at microwave frequencies have been measured (Cimino, 1982), direct extrapolation of these results into the millimeter-wave region can lead to ambiguous results.

This paper describes the methodology and the results of laboratory measurements of the millimeter-wave properties of liquid sulfuric acid. These measurements represent the first time that measurements of the millimeter-wave dielectric property of liquid sulfuric acid have been reported.

In this paper, we describe measurements conducted at 30-40 and 90-100 GHz, using two different concentrations of liquid H_2SO_4. In addition, the measured data is used to compute the expected opacity of H_2SO_4 condensates and their effects on the millimeter-wave emission from Venus.

II. Experimental Approach

The approach used in the measurement of the dielectric properties of liquid sulfuric acid at millimeter-wave frequencies is similar to that described by Moore et al. (1991). The experiment employs a free space transmission setup as indicated in Figure 1. In this configuration, the sample is placed between the transmitting and receiving antennas. In addition, optical lenses are used to focus the energy on the surface of the sample. The lenses and the two horn antennas are mounted on an adjustable rail to allow accurate positioning of these components with respect to the sample. Although the sample holder is designed to rotate to change the incidence angle of the transmitted wave, our measurements were performed at a normal incidence with respect to the sample.

In order to use this system for measuring the complex dielectric constant of liquids, a suitable cell had to be designed to hold the liquid sulfuric acid and to minimize the reaction of the acid with the cell walls. A sketch of the cell used is shown in Figure 2 where the cell walls are manufactured from high grade Teflon. The thickness of the cell walls and the liquid sample are chosen so

that an adequate signal level can be measured by the receiving antenna. A thickness of 1270 μm is chosen as an appropriate value for the walls and liquid sample. In addition, the variation in the thickness of the cell walls is minimized in order to insure a uniform sample thickness (±25.4 μm is achieved).

A block diagram of the electrical components used to measure the dielectric constant of liquid sulfuric acid between 90-100 GHz is shown in Figure 3. A similar system employing different antennas and lenses along with the appropriate power source is used for frequencies between 30.0 and 40.0 GHz. In both configurations, the system employs a digital computer to automate the measurement process and to control the Hewlett-Packard 8510 network analyzer used to measure the transmission coefficient of the liquid sample.

III. Experimental Procedure

The first step in the measurement process is the calibration of the system (without the sample). In addition, a check on the accuracy of the calibration process is performed by measuring the dielectric constant of a single sheet of material and comparing the measured values with published data. Once the calibration is satisfactory, the filled cell is mounted and measurement of the transmission coefficient of the liquid , $(S_{21})_{measured}$, as function of frequency is performed. The results of such measurements are then stored on a magnetic disk for later analysis.

As stated earlier, the measurement of the complex permittivity ($\epsilon_r = \epsilon'_r - j\epsilon''_r$) of liquid sulfuric acid was performed at two different frequency bands covering 30-40 and 90-100 GHz. The measurements of the complex dielectric constant of two samples of liquid sulfuric acid having 99% and 85% concentration by weight were performed. The latter concentration was equivalent to the estimated concentration of sulfuric acid in the clouds of Venus. In addition, the measurement of the dielectric constant of distilled water was performed in order to check the accuracy of our measurement process. In this case, a close agreement between our measurements and those previously reported (Oguchi, 1983) was obtained.

IV. Determination of ϵ_r

The determination of the complex dielectric constant of the liquid under test requires careful characterization of the geometry of the cell used and the determination of the theoretical transmission coefficient of that cell. A sketch of the liquid cell used in our setup is shown in Figure 4 where medium I and III denote the teflon walls of thickness d while medium II represents the liquid under test with thickness t. For the geometry shown in Figure 4, a composite scattering matrix representing the three media and the corresponding interfaces can be written as,

$$[S]_T = [S]_{12}[S]_I[S]_{23}[S]_{II}[S]_{34}[S]_{III}[S]_{45} \qquad (1)$$

where $[S]_T$ is a 2x2 matrix relating the incoming and outgoing wave amplitudes in medium 1 and 5 as shown Figure 4. Another important quantity is the propagation constant of an electromagnetic wave in medium i which can be expressed as,

$$k_i = 2\pi f \frac{\sqrt{\mu_{ri}\epsilon_{ri}}}{c} \qquad (2)$$

where f denotes the frequency, c is the speed of light in free space and ϵ_{ri} and μ_{ri} are respectively the relative complex permittivity and permeability of medium i. These two complex quantities can be expressed as,

$$\mu_{ri} = \mu'_{ri} - j\mu''_{ri} \qquad (3)$$

and

$$\epsilon_{ri} = \epsilon'_{ri} - j\epsilon''_{ri} . \qquad (4)$$

Since liquid sulfuric acid does not posses magnetic properties, μ_{ri} is equal to μ_o.

The composite scattering matrix $[S]_T$ can then be written as a function of the propagation constants of the three media and their respective thicknesses. Since the dielectric constant of Teflon is well known ($\epsilon_{rI} = \epsilon_{rIII} = 2.0 - j.02$), $[S]_T$ can then be written as a function $\mathcal{F}$ such that,

$$[S]_T = \mathcal{F}(k_{II}, t, d) \qquad (5)$$

where k_{II} is the propagation constant in medium II as expressed in equation (2).

Once $[S]_T$ has been determined, one can solve for the propagation constant of medium II (k_{II}) by minimizing,

$$(S_{21})_{measured} - (S_{21})_T \qquad (6)$$

where $(S_{21})_{measured}$ is the measured transmission coefficient of the filled cell while $(S_{21})_T$ is the theoretically calculated transmission coefficient obtained from the matrix $[S]_T$. This minimization process is carried out using a root finder program based on Newton's method and an initial guess for k_{II}. Once a satisfactory value of k_{II} has been reached in accordance with (6), the complex dielectric constant of the liquid under test can be determined using,

$$\epsilon_{rII} = (k_{II}/k_o)^2 \qquad (7)$$

where k_o denotes the propagation constant in free space.

V. Experimental Results

The results of the measurements of the complex dielectric constant of liquid sulfuric acid at frequencies between 30.0 and 40.0 GHz are shown in Figures 5 and 6. Figure 5 shows the real part of the relative dielectric constant (ϵ'_{rII}) as function of frequency for 99.0% and 85.0% concentrations (by weight) of sulfuric acid in addition to ϵ'_{rII} for water (room temperature). Figure 6 shows the imaginary part of ϵ_{rII} (ϵ''_{rII}) as function of frequency for the same liquids.

Similarly, the results of the measurement of the complex dielectric constant at 90.0-100.0 GHz are shown in Figures 7 and 8. The error bars shown in these four figures represent $\pm 1\sigma$ variation in the calculated values of ϵ'_{rII} and ϵ''_{rII} resulting from uncertainties in the thickness t of $\pm 25.4\,\mu m$. Hence, these error bars do not include uncertainties due to instrumental errors which are on the order of ±3% of the reported mean values.

In order to apply the measured data in modeling the emission from the atmosphere of Venus, a relationship between the complex dielectric constant, physical parameters of the condensate (size and mass content) and the expected absorptivity of such a condensate is needed. Regarding the physical parameters of the condensate, extensive studies have been performed using data from several entry probes (Knollenberg and Hunten, 1980). Droplets sizes of 25 microns with an approximate mass content of 50 mg/m^3 provide a conservative upper limit for the physical parameters of the cloud condensate. As a result, the expected absorptivity can be evaluated using a Rayleigh absorption model (that is , $|(\epsilon_r)^{1/2}\chi| < 1$, where $\chi = 2\pi r(\epsilon'_r)^{1/2}/\lambda$ and r is the radius of the droplets, (Ulaby,1981)) where the absorption coefficient, α, can be expressed as,

$$\alpha = \frac{246 M \epsilon''_r}{\rho\lambda[(\epsilon'_r+2)^2+(\epsilon''_r)^2]} \ (\mathrm{dB/km}) \qquad (8)$$

where ρ is the density of the liquid and M is the bulk density of the clouds in the same units, λ is the wavelength in km and ϵ'_r and ϵ''_r are, respectively, the real and imaginary parts of the complex dielectric constant of the liquid. (Note, for example, that an attenuation constant or absorption coefficient or absorptivity of 1 Neper km^{-1} = 2 optical depths per km (or km^{-1})= 8.686 dB km^{-1}, where the first notation is the natural form used in electrical engineering, the second is the usual form in physics and astronomy, and the third is the common (logarithmic) form. The third form is often used in order to avoid a possible factor-of-2 ambiguity in meaning).

The calculated values of the absorption coefficient of liquid sulfuric acid for 85% and 99% concentration by weight (in addition to those for water) are shown in Figures 9 and 10. In these figures, the absorption of H_2SO_4 and H_2O droplets have been calculated for the same volume density (M/ρ ratio is constant for both liquids). A close examination of these results indicate that the expected absorption for 85% concentrated sulfuric acid droplets is at least 20% higher than that expected from water. This indicates that the absorptivity of sulfuric acid may have an effect on the variation of the millimeter-wave emission from Venus.

VI. Discussion

The key result of our work has been the determination of the complex dielectric constant of liquid sulfuric acid at the concentration expected for the clouds of Venus. Our results show that the expected absorption of liquid H_2SO_4 is at least 20% higher than that of water condensate. Thus the absorption from liquid sulfuric acid may affect the millimeter-wave emission of Venus. In order to determine the effect of H_2SO_4 droplets on the emission of Venus, our data has been incorporated into a radiative transfer model of the atmosphere of Venus. This model calculates the effects of several constituents (gaseous SO_2, CO_2 and H_2O) on the brightness temperature of Venus at millimeter wavelengths. Although the absorptivities of some of the constituents have not been measured at millimeter wavelengths, extensive analytical calculations regarding their absorptivities have been reported. In addition, the absorption of gaseous sulfuric acid is not included in our model since no measured or calculated data have been reported at these high frequencies.

Preliminary results from the radiative transfer model indicate that liquid H_2SO_4 does indeed affect the brightness temperature of Venus at 95 GHz. A decrease of 2 K is indicated for a uniform cloud layer in the 48-50 km altitude range similar to that described by Knollenberg and Hunten (1980). This decrease in brightness temperature is comparable with that attributable to gaseous SO_2 (SO_2 is assumed to be uniformly mixed below 48 km altitude and exponentially decreasing above). However, this 2 K variation in brightness temperature is much less than the observed variation in the millimeter-wave emission of Venus. Recently, de Pater (1991) reported observing a variation of 30 K in the brightness temperature of Venus at 112 GHz.

In order to determine which constituents are responsible for the reported variations in the emission of Venus, a complete knowledge of the millimeter-wave properties of all constituents (especially gaseous H_2SO_4) is necessary.

VII. Conclusion

Laboratory measurements of the complex dielectric constant of liquid sulfuric acid at 30-40 and 90-100 GHz have been performed on two different samples of H_2SO_4 with 85% and 99% concentration by weight. Using the measured data and the physical parameters of sulfuric acid condensate in the clouds of Venus, the absorptivity of H_2SO_4 condensate has been determined.

The calculated absorptivity of liquid sulfuric acid has been incorporated into a radiative transfer model of Venus in order to determine the effects of H_2SO_4 droplets on the variability in the millimeter-wave emission from Venus. The results of our model indicate that the cloud condensate does have an effect on the emission of Venus. However, the calculated decrease in brightness temperature is well below the observed decrease in brightness temperature (de Pater, 1991). As a result, this observed variability may not be completely due to sulfuric acid droplets.

Other constituents such as gaseous H_2SO_4 may also affect the observed variations in the brightness temperature. The effect of this constituent is not fully known since no measurement of the absorption of gaseous sulfuric acid have been performed at millimeter-wave frequencies. Hence, one can only speculate whether this variability can be completely due to liquid sulfuric acid.

Currently, measurements of the absorption of gaseous sulfuric acid and SO_2 at millimeter-wavelengths are being performed under Venus-like conditions. The results from our measurements will be incorporated in our model in order to determine the effects of these constituents on the observed variability in the brightness temperature of Venus.

Acknowledgments. We thank Ms. Anita MacDonald and Drs. Tom Wells and Rick Moore of the Georgia Tech Research Institute for providing facilities and equipment assistance for the experiment. We also would like to thank Ms. Joanna Joiner for her valuable comments regarding the radiative transfer model of Venus. This work was supported by the Planetary Atmospheres Program of the National Aeronautics and Space Administration under grant NAGW-533.

References

Cimino, J. B., The composition and vertical structure of the lower cloud deck on Venus, Icarus, 51, 334-357, 1982.

de Pater, I., F. P. Schloerb, and A. Rudolph, Venus images with the hat creek interferometer in the j-1-0 CO line, Icarus, in press (1991).

Ho, W., I. A. Kaufman, and P. Thaddeus, Laboratory measurements of microwave absorption in models of the atmosphere of Venus, J. Geophys. Res., 71, 5091-5108, 1966.

Knollenberg, R. G., and D. M. Hunten, The microphysics of the clouds of Venus: Results of the Pioneer Venus particle size spectrometer experiment, J. Geophys. Res., 85, 8039-8058, 1980.

Moore, R., A. MacDonald, and H. Ross Moroz, Permittivity of fiber-polymer composite: A study to determine effects of environment, Microwave Journal, Vol. 34, no.2, 1991 (in press).

Ogushi, 1, Electromagnetic wave propagation and scattering in rain and other hydrometers, Proceedings of the IEEE, 71, 1029-1032, 1983.

Steffes, P. G., and V. R. Eshleman, Sulfuric acid vapor and other cloud-related gases in the Venus atmosphere: Abundances inferred from observed radio opacity, Icarus, 51, 322-333, 1982.

Steffes, P. G. , Laboratory measurements of the microwave opacity and vapor pressure of sulfuric acid vapor under simulated conditions for the middle atmosphere of Venus, Icarus, 64, 576-585, 1985.

Steffes, P. G., M. J. Klein, and J. M. Jenkins, Observation of the microwave emission of Venus from 1.3 to 3.6 cm, Icarus, 84, 83-92, 1990.

Ulaby, T. F., R. K. Moore, and A. K. Fung, Microwave Remote Sensing: Active and Passive, Volume 1, Addison-Wesley publishing company, Massachusetts, 1981.

A. K. Fahd and P. G. Steffes, School of Electrical Engineering, Georgia Institute of Technology, Atlanta, Georgia, 30332.

Fahd and Steffes: Dielectric constant of H_2SO_4

Fahd and Steffes: Dielectric constant of H_2SO_4

Fig. 1. Sketch of free space measurement system.

Fig. 2. Sketch of the liquid cell used in the free space measurement of the dielectric constant of sulfuric acid.

Fig. 3. Block diagram of the free space measurement setup, as configured for measurements of the millimeter-wave complex dielectric constant of liquid sulfuric acid.

Fig. 4. Detailed sketch of the liquid cell representing various media and their respective interfaces.

Fig. 5. The measured real part of the complex dielectric constant of water and sulfuric acid for frequencies between 30 and 40 GHz at room temperature. Error bars indicate $\pm 1\sigma$ variation in the measured quantities about the mean values.

Fig. 6. The measured imaginary part of the complex dielectric constant of water and sulfuric acid for frequencies between 30 and 40 GHz at room temperature. Error bars indicate $\pm 1\sigma$ variation in the measured quantities about the mean values.

Fig. 7. The measured real part of the complex dielectric constant of water and sulfuric acid for frequencies between 90 and 100 GHz at room temperature. Error bars indicate $\pm 1\sigma$ variation in the measured quantities about the mean values.

Fig. 8. The measured imaginary part of the complex dielectric constant of water and sulfuric acid for frequencies between 90 and 100 GHz at room temperature. Error bars indicate $\pm 1\sigma$ variation in the measured quantities about the mean values.

Fig. 9. Comparison of attenuation (dB/km) from an 85% (by weight) sulfuric acid solution with that from water droplets for a particular volume fraction (volume of particles/total volume = 2.82×10^{-8}) for frequencies between 30 and 40 GHz.

Fig. 10. Comparison of attenuation (dB/km) from an 85% sulfuric acid solution with that from water droplets for a particular volume fraction (volume of particles/total volume = 2.82×10^{-8}) for frequencies between 90 and 100 GHz.

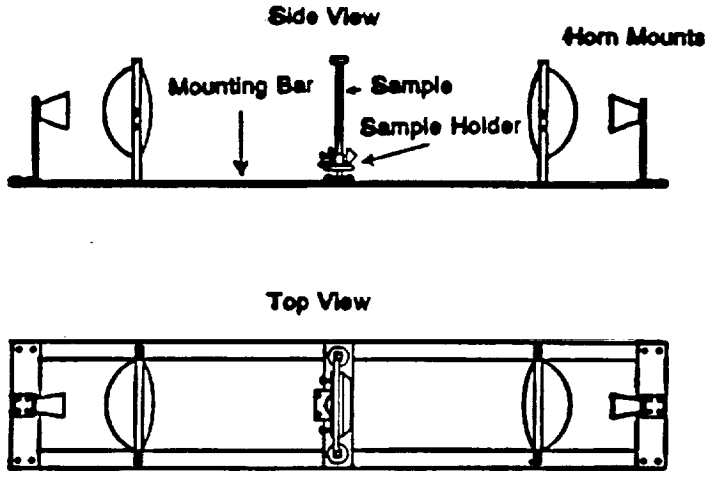

FAHD AND STEFFES, FIGURE 1

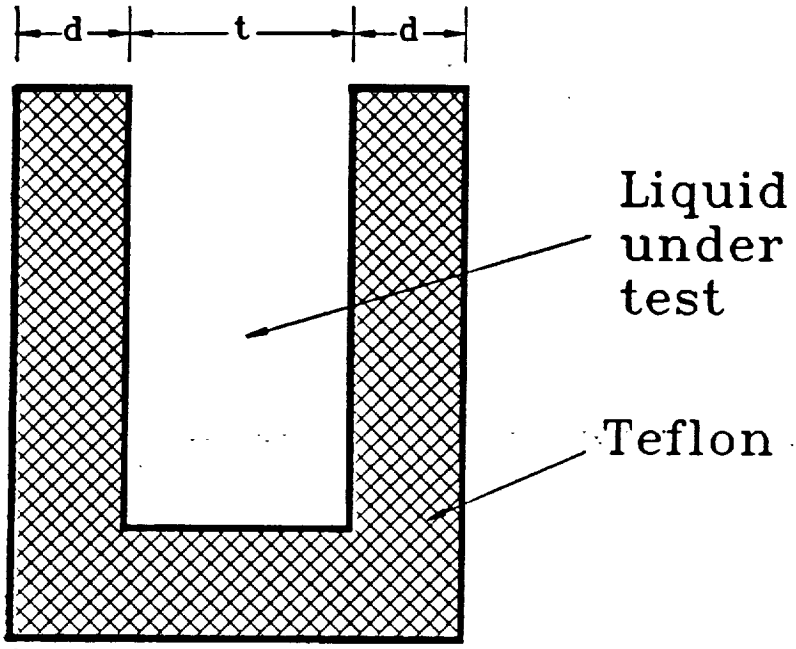

FAHD ANS STEFFES, FIGURE 2

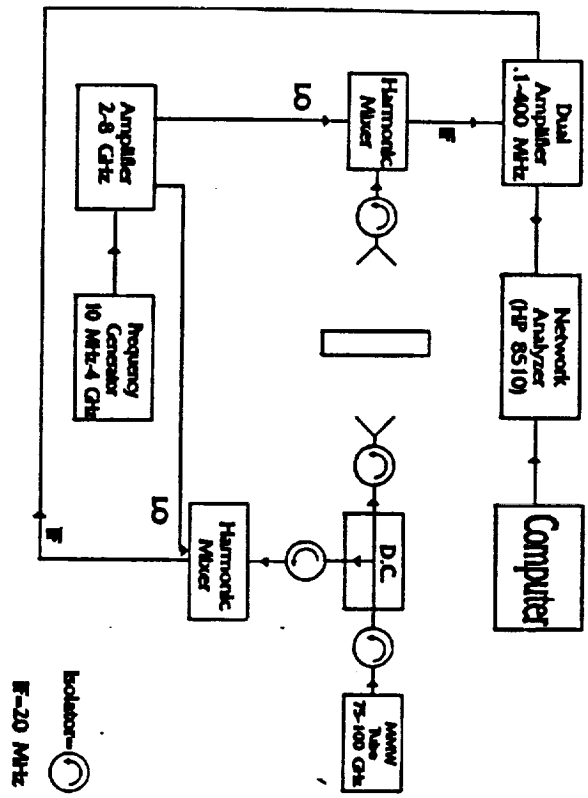

FAHD AND STEFFES, FIGURE 3

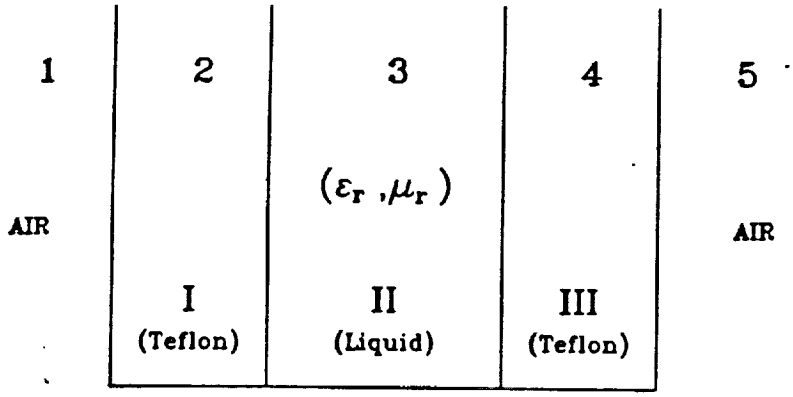

FAHD AND STEFFES, FIGURE 4

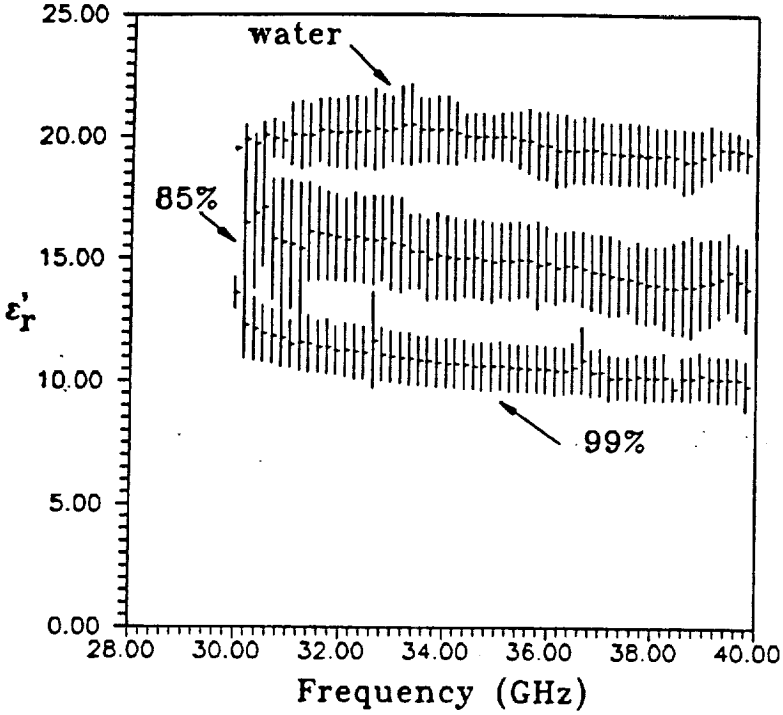

FAHD AND STEFFES, FIGURE 5

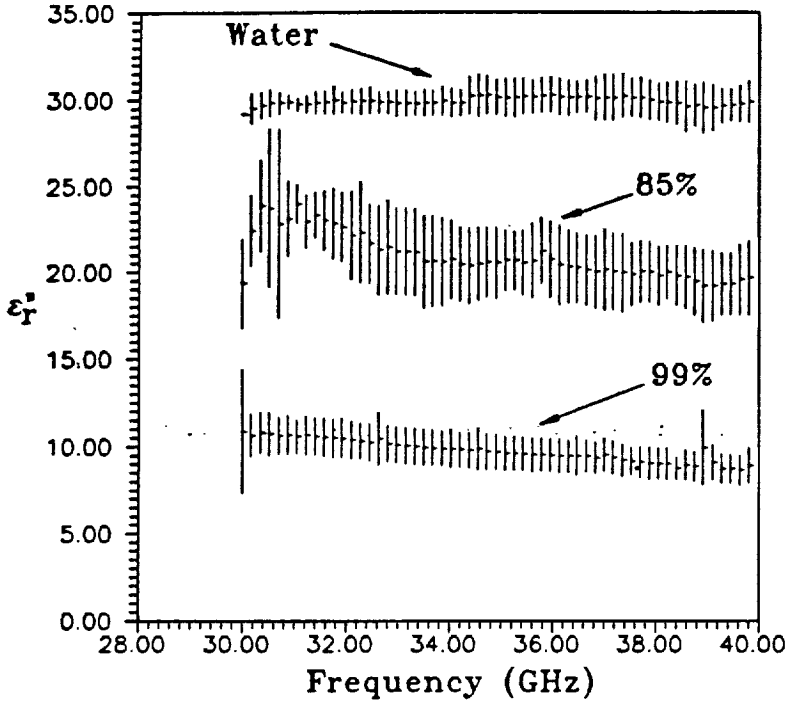

FAHD AND STEFFES, FIGURE 6

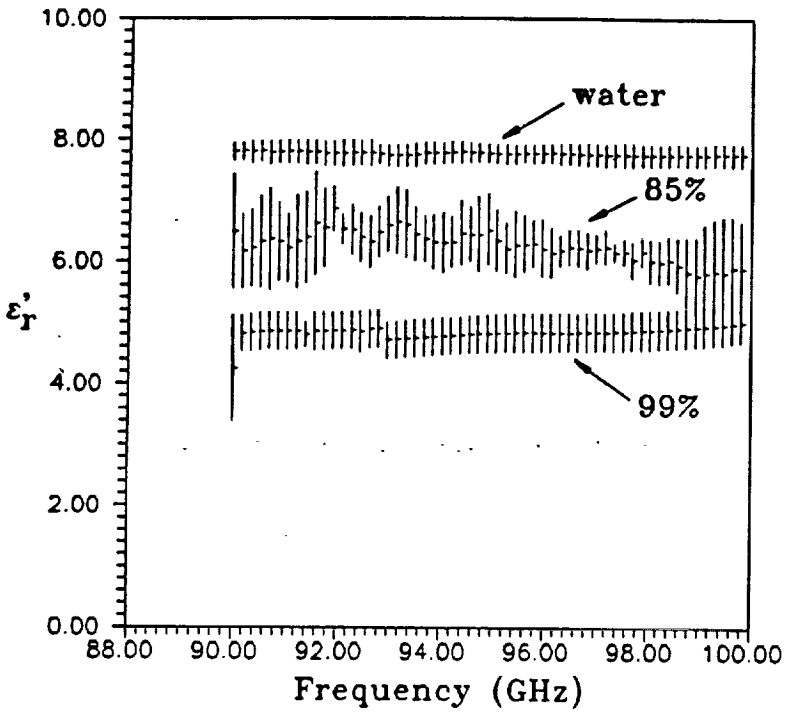

FAHD ANS STEFFES, FIGURE 7

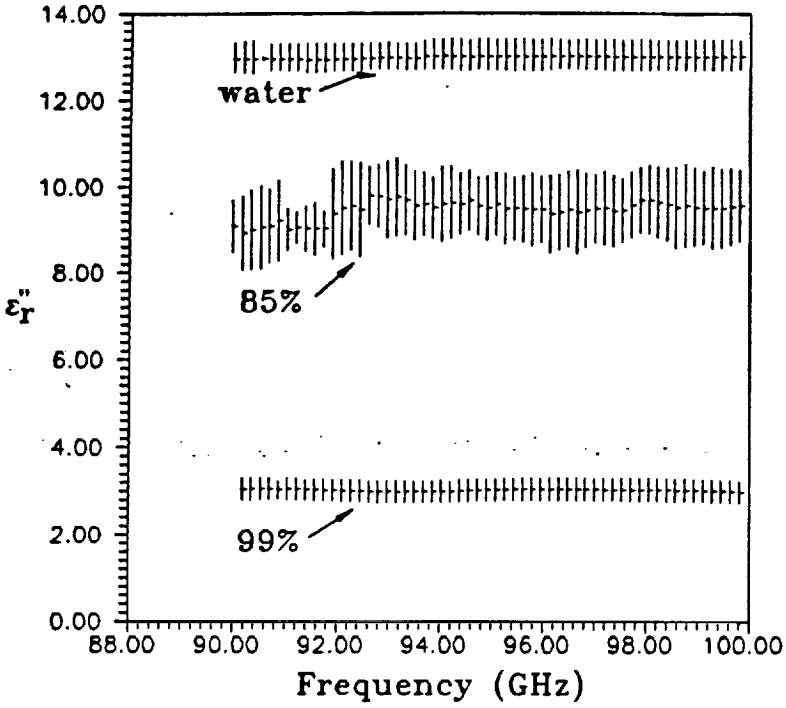

FAHD AND STEFFES, FIGURE 8

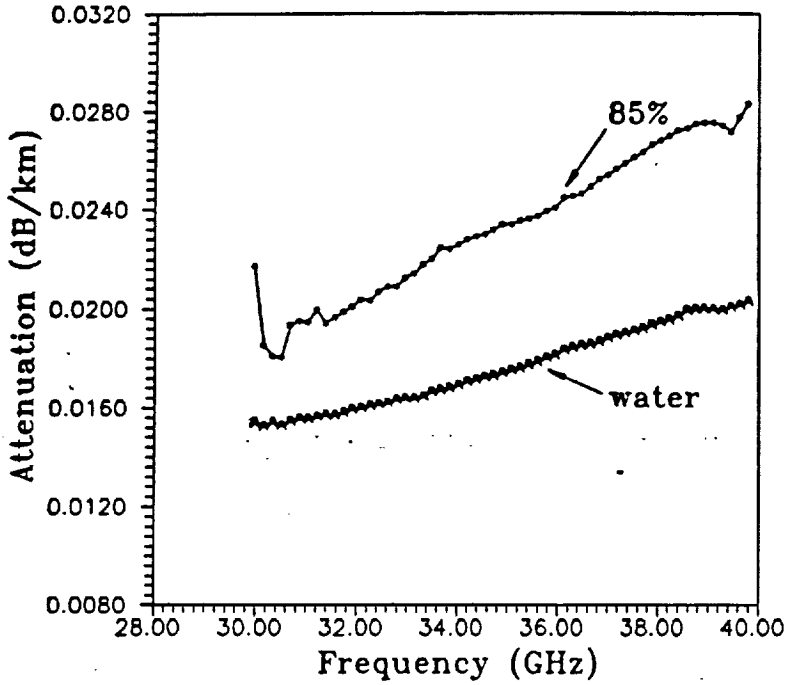

FAHD AND STEFFES, FIGURE 9

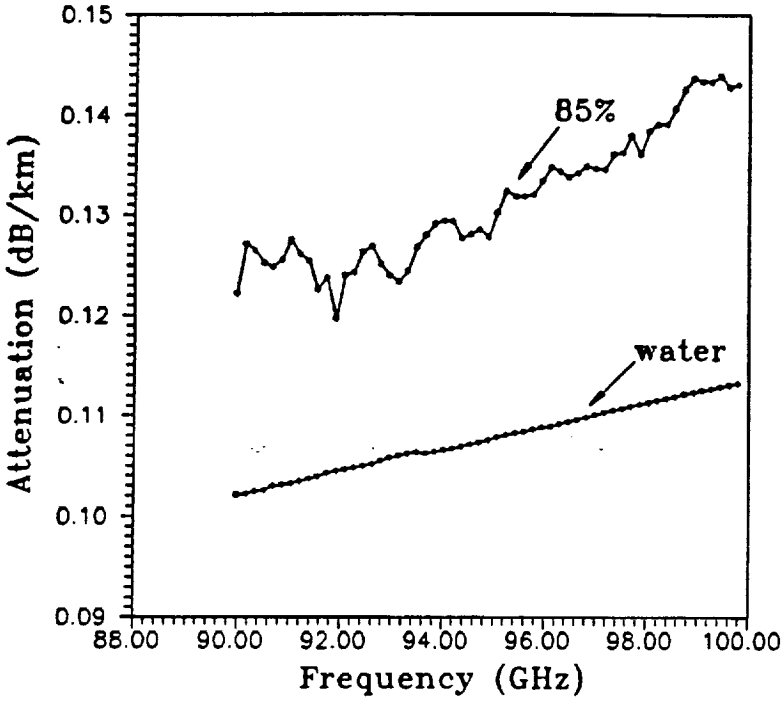

FAHD AND STEFFES, FIGURE 10